Direct observation of the Migdal effect induced by neutron bombardment

Qian LIU (on behalf of **MARVEL** group)

Migd**A**l p**R**ocess **V**alidation by n**E**utrua**L** scattering

University of Chinese Academic of Sciences

IDM 2026, Zaragoza

Outline

- Motivation
- MARVEL experiment
- Detector design&performance
- Beam experiments
- Event selection
- Background analysis
- Results
- Detector upgrade
- Summary & outlook

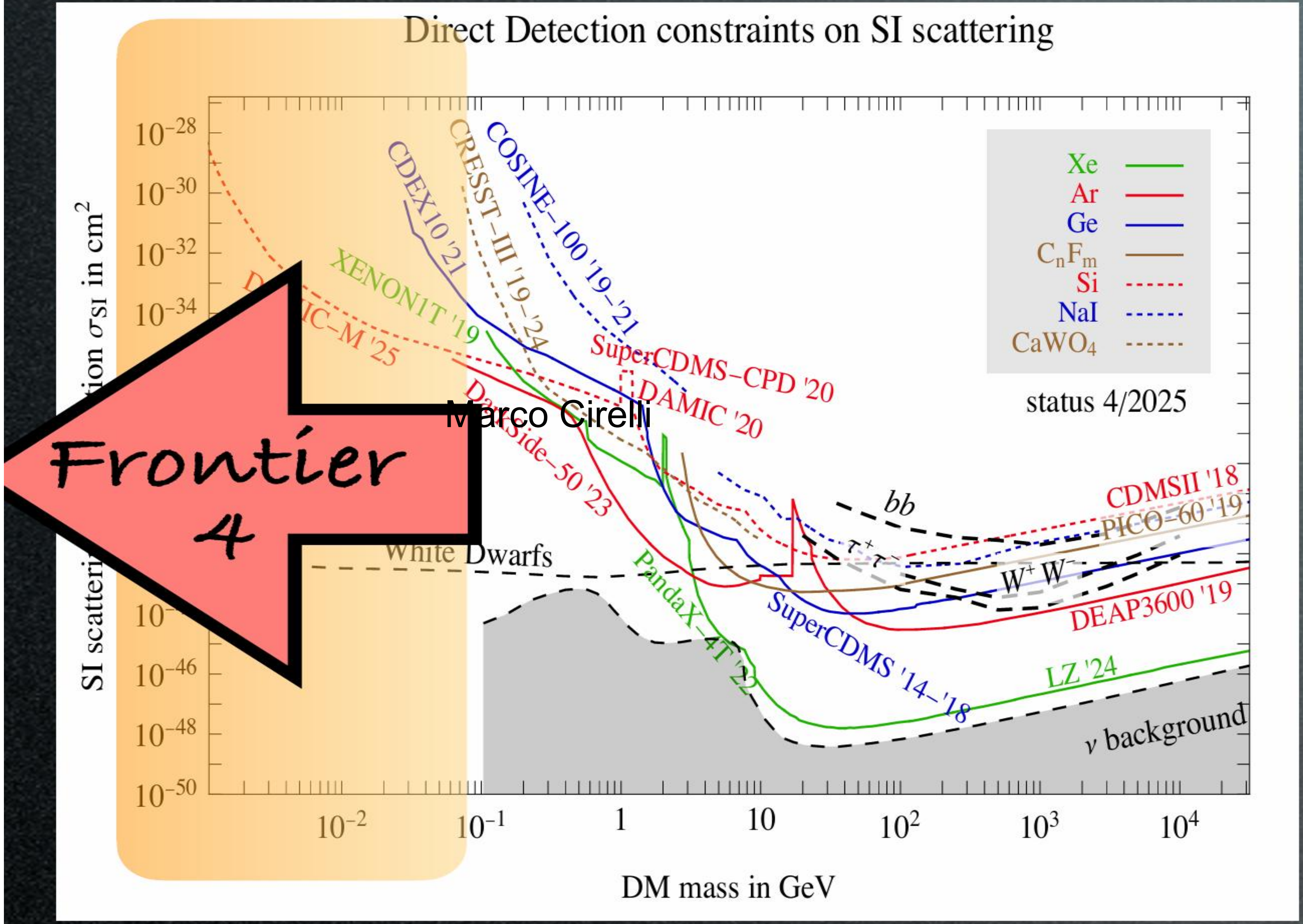

M. Cirelli, A. Strumia, J. Zupan 'Dark Matter', 2406.01705

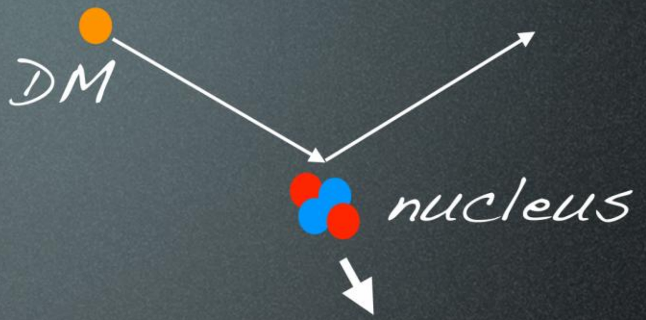

deposited energy is **below threshold** for typical nuclear recoil experiments

- electron recoil signal
- Migdal effect (?)
- new experimental strategies

Marco Cirelli, IDM 2026

Migdal effect

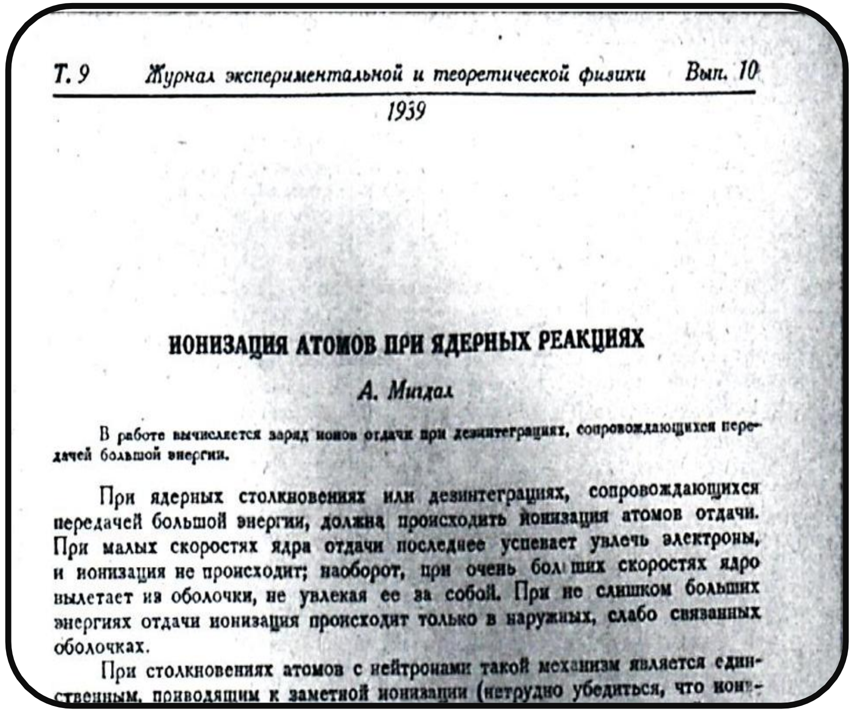

Т. 9 Журнал экспериментальной и теоретической физики Вып. 10

1939

ИОНИЗАЦИЯ АТОМОВ ПРИ ЯДЕРНЫХ РЕАКЦИЯХ

А. Мигдал

В работе вычисляется заряд ионов отдачи при дезинтеграциях, сопровождающихся передачей большой энергии.

При ядерных столкновениях или дезинтеграциях, сопровождающихся передачей большой энергии, должна происходить ионизация атомов отдачи. При малых скоростях ядра отдачи последнее успевает увлечь электроны, и ионизация не происходит; наоборот, при очень больших скоростях ядро вылетает из оболочки, не увлекая ее за собой. При не слишком больших энергиях отдачи ионизация происходит только в наружных, слабо связанных оболочках.

При столкновениях атомов с нейтронами такой механизм является единственным, приводящим к заметной ионизации (нетрудно убедиться, что ион-

- First predicted by Migdal in 1939-1940
- describes a physical phenomenon where a suddenly accelerated atomic nucleus transfers energy to its orbital electrons through a rapid change in the electric field, causing the electrons to become ionized or excited.
- observed in radioactive decays in the 70's.
- **but not observed in nuclear scattering.**

PhysRevLett.108.243201 (2012)

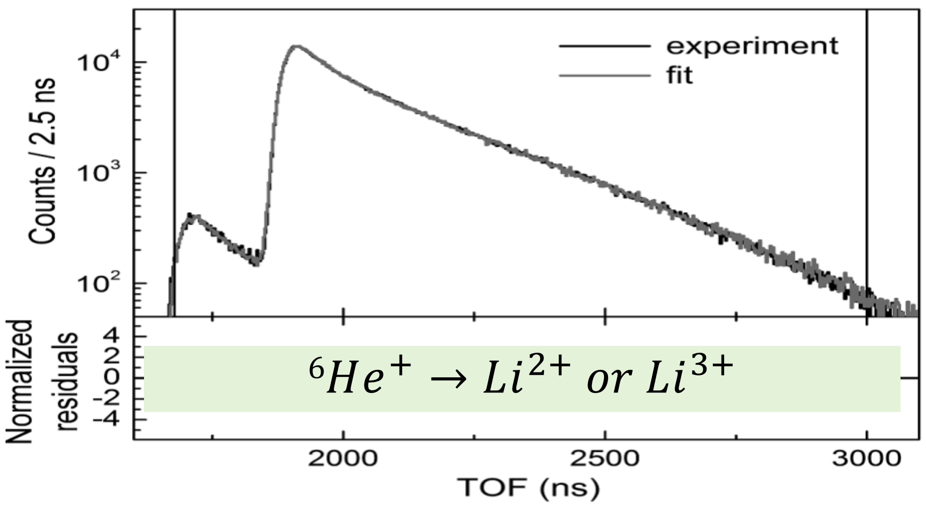

PhysRevC.11.1740 (1975)

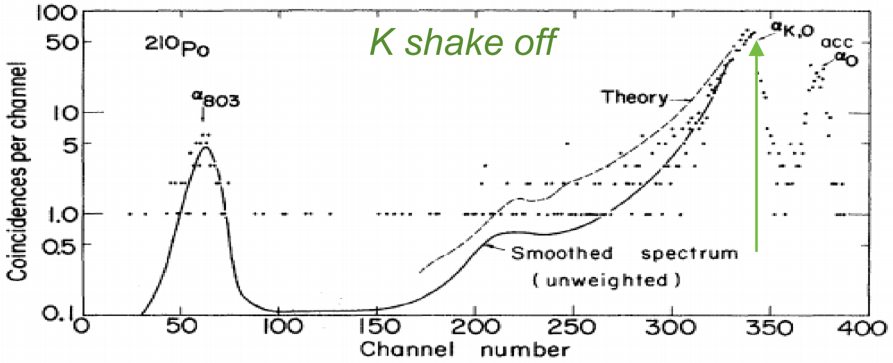

β deacy

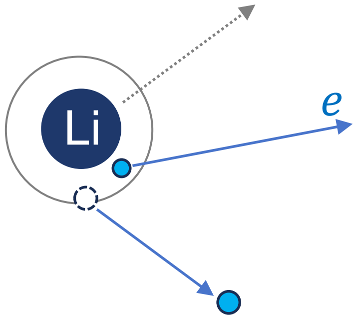

α decay

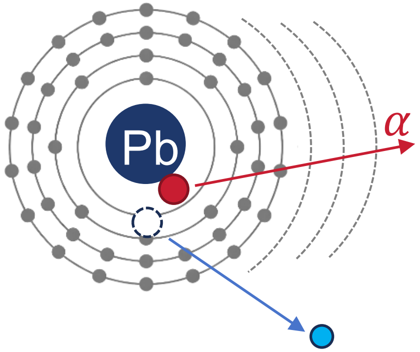

Migdal effect

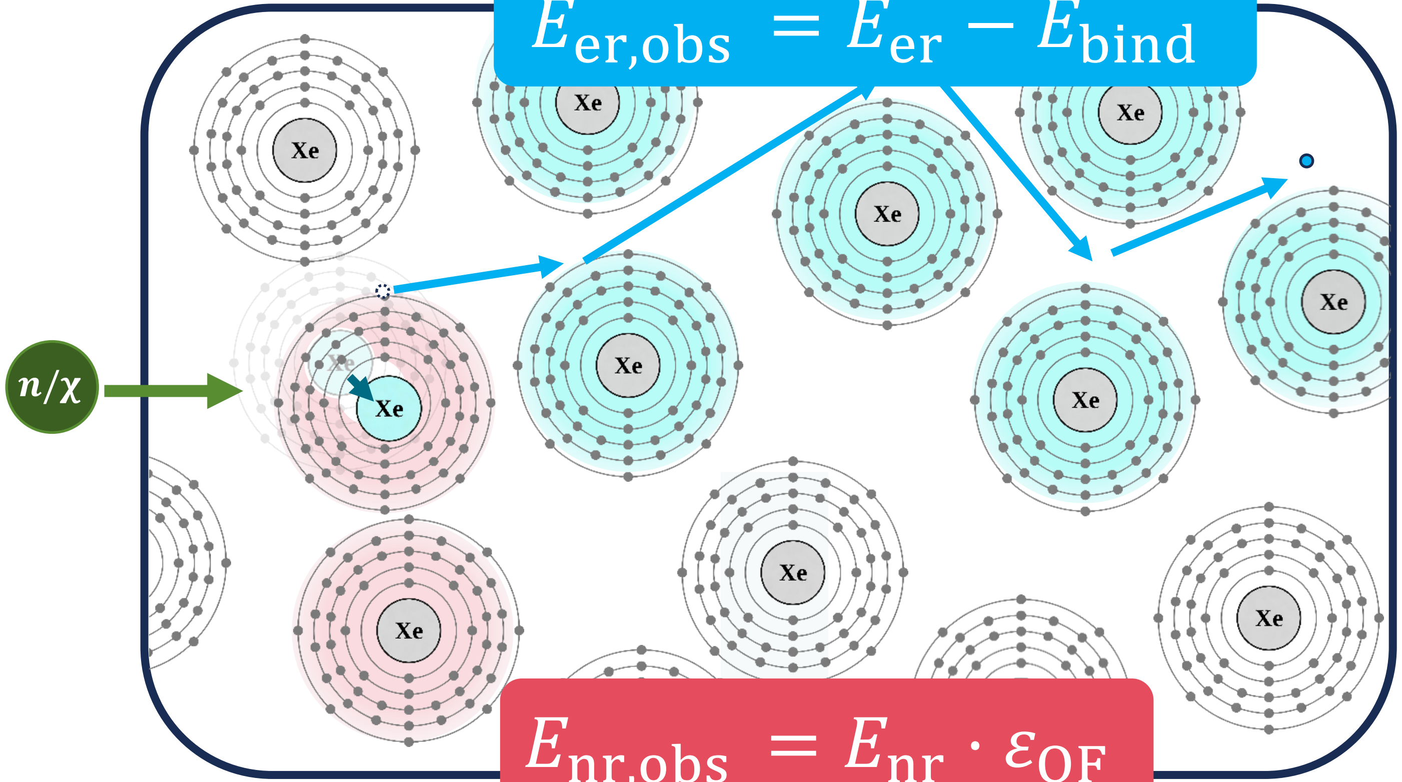

$$E_{\mathrm{er,obs}} = E_{\mathrm{er}} - E_{\mathrm{bind}}$$

$$E_{\mathrm{nr,obs}} = E_{\mathrm{nr}} \cdot \varepsilon_{\mathrm{QF}}$$

$$E_{\mathrm{det}} = E_{\mathrm{er,obs}} + E_{\mathrm{nr,obs}} + \ldots$$

Z.Liu, [Phd thesis], 2022

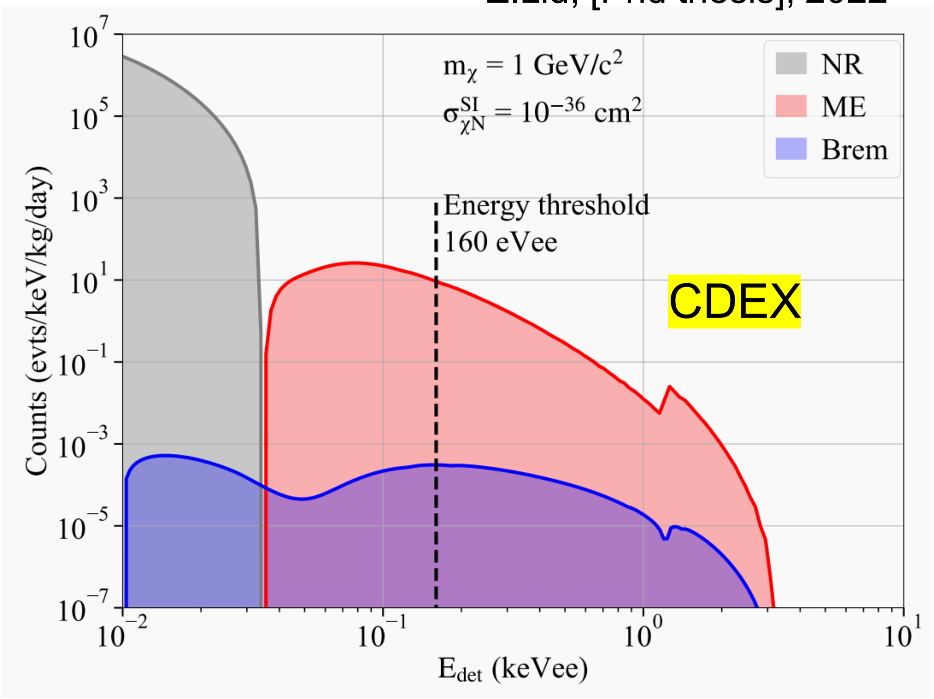

Nuclear recoils below the threshold, which are otherwise undetectable, become observable through Migdal electron energy deposition.

Sub-GeV DM searches

SuperCDMS Collaboration. Inelastic DM search with CDMSlite R3 [EB/OL]. 2025[2026-03-02].

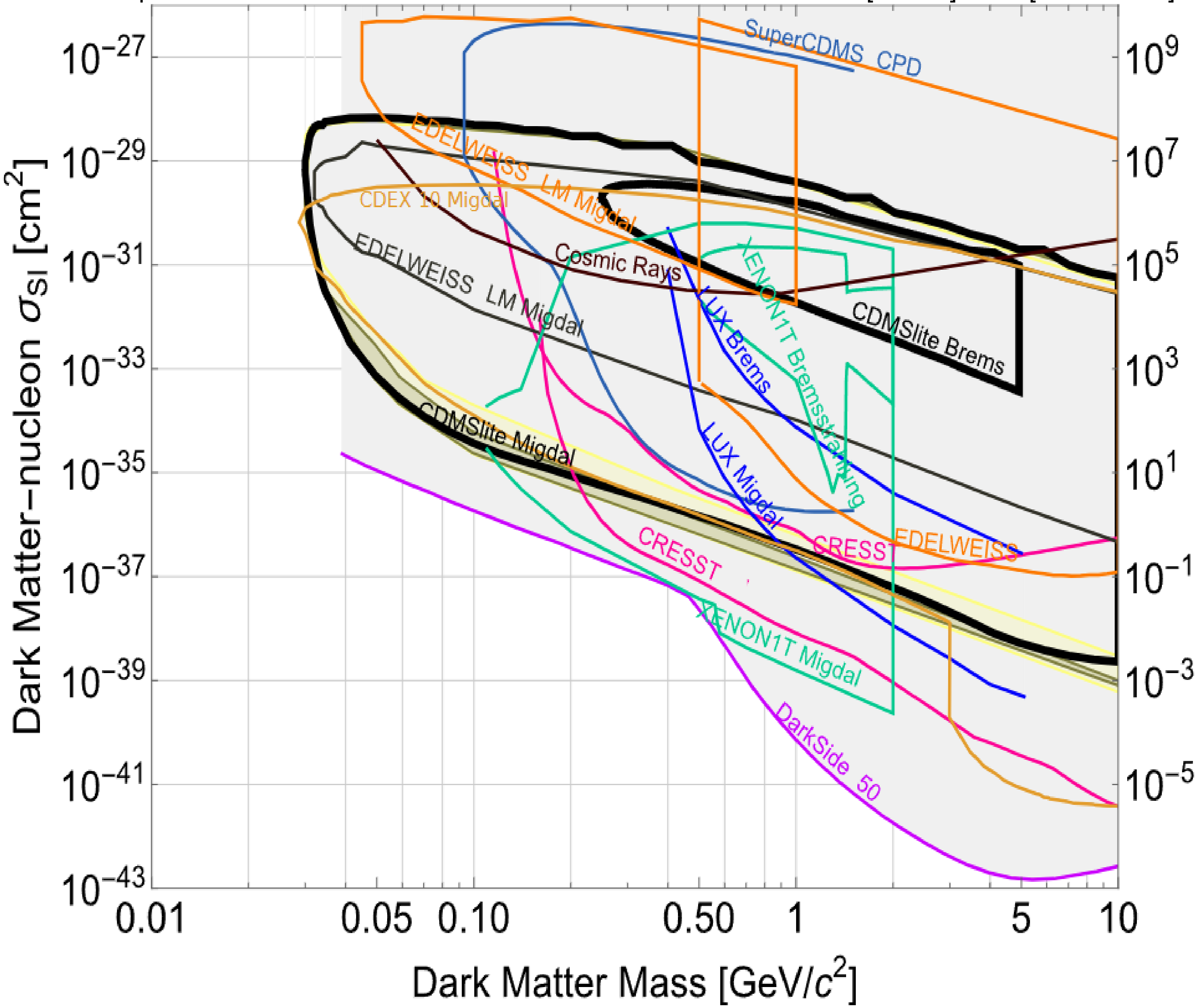

Search for Light Dark Matter Interactions Enhanced by the Migdal Effect or Bremsstrahlung in XENON1T #1
XENON Collaboration • E. Aprile (Columbia U.) et al. (Jul 30, 2019)
Published in: Phys.Rev.Lett. 123 (2019) 24, 241803 • e-Print: 1907.12771 [hep-ex]
pdf DOI cite claim reference search 329 citations

Search for new physics in low-energy electron recoils from the first LZ exposure #1
LZ Collaboration • J. Aalbers (SLAC and Stanford U., Phys. Dept. and KIPAC, Menlo Park) et al. (Jul 28, 2023)
Published in: Phys.Rev.D 108 (2023) 7, 072006 • e-Print: 2307.15753 [hep-ex]
pdf links DOI cite datasets claim reference search 73 citations

Search for Dark-Matter–Nucleon Interactions with a Dark Mediator in PandaX-4T #1
PandaX Collaboration • Di Huang (Shanghai Jiao Tong U.) et al. (Aug 3, 2023)
Published in: Phys.Rev.Lett. 131 (2023) 19, 191002 • e-Print: 2308.01540 [hep-ex]
pdf DOI cite claim reference search 51 citations

Results of a Search for Sub-GeV Dark Matter Using 2013 LUX Data #1
LUX Collaboration • D.S. Akerib (Case Western Reserve U. and SLAC and KIPAC, Menlo Park) et al. (Nov 27, 2018)
Published in: Phys.Rev.Lett. 122 (2019) 13, 131301 • e-Print: 1811.11241 [astro-ph.CO]
pdf DOI cite claim reference search 213 citations

Search for Dark-Matter–Nucleon Interactions via Migdal Effect with DarkSide-50 #1
DarkSide Collaboration • P. Agnes (Royal Holloway, U. of London) et al. (Jul 25, 2022)
Published in: Phys.Rev.Lett. 130 (2023) 10, 10 • e-Print: 2207.11967 [hep-ex]
pdf links DOI cite claim reference search 107 citations

Search for low-mass dark matter via bremsstrahlung radiation and the Migdal effect in SuperCDMS #1
SuperCDMS Collaboration • M.F. Albakry (British Columbia U. and TRIUMF) et al. (Feb 17, 2023)
Published in: Phys.Rev.D 107 (2023) 11, 2023 • e-Print: 2302.09115 [hep-ex]
pdf links DOI cite claim reference search 43 citations

Search for sub-GeV dark matter via the Migdal effect with an EDELWEISS germanium detector with NbSi transition-edge sensors #2
EDELWEISS Collaboration • E. Armengaud (IRFU, Saclay) et al. (Mar 8, 2022)
Published in: Phys.Rev.D 106 (2022) 6, 062004 • e-Print: 2203.03993 [astro-ph.GA]
pdf DOI cite claim reference search 66 citations

XENON/LZ/PandaX/CDEX/DarkSide-50/SuperCDMS/EDELWEISS/LUX…

Migdal effect detection Experiments

Phys. Rev. D,107, 035032

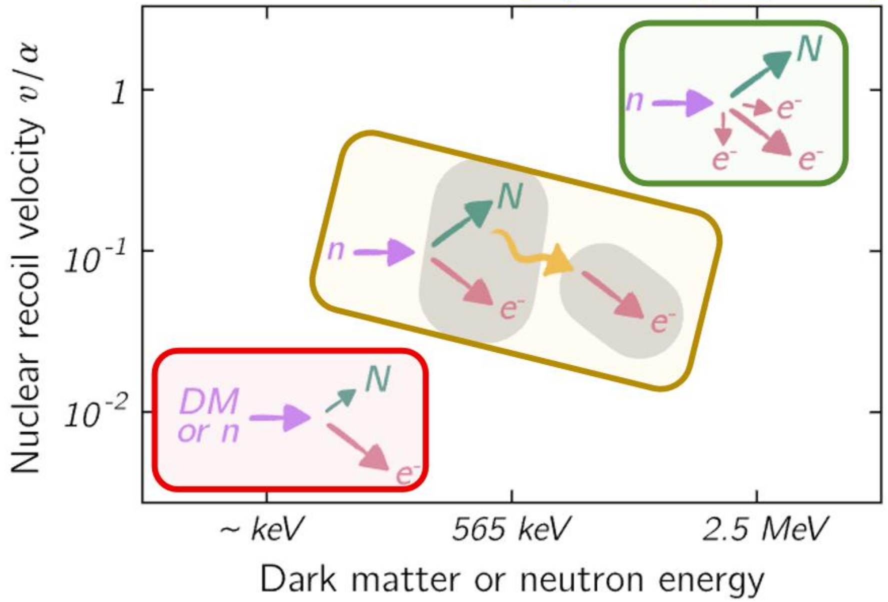

MIGDAL

arXiv, 2022, 08284

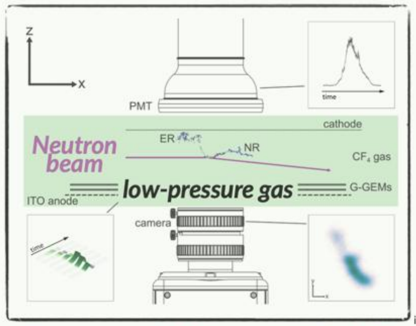

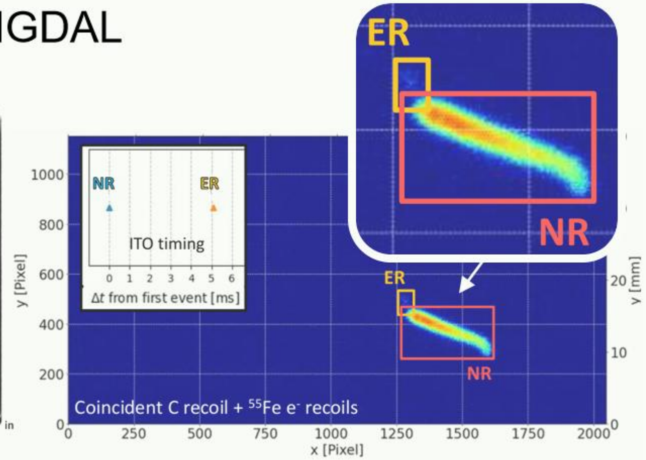

$E_{\mathrm{neutron}} \sim 2500 - 15000$ keV

Phys. Rev. D, 109(5), L051101

LXe

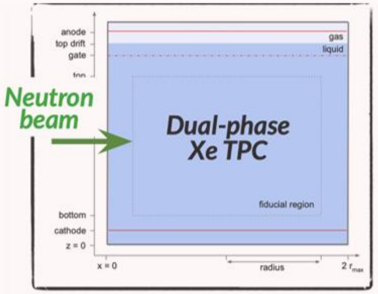

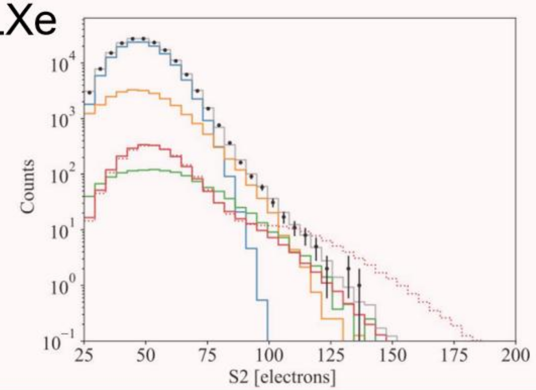

$E_{\mathrm{neutron}} \sim 15$ keV

PTEP,2021(1),013C01

MIRACLUE

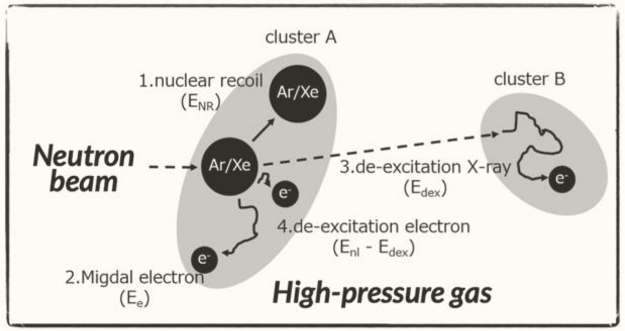

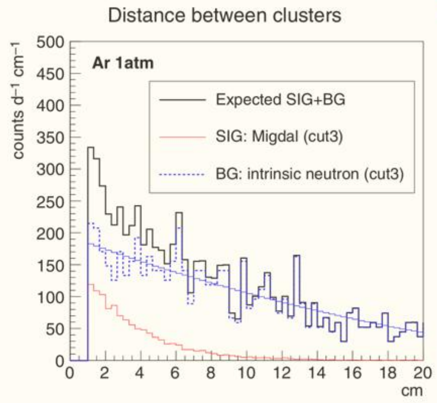

$E_{\mathrm{neutron}} \sim 500$ keV

MARVEL Experiment-Detector

GMCP

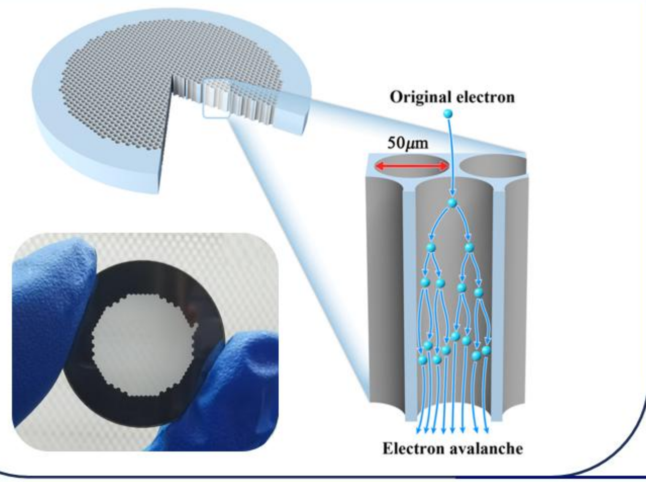

Topmetal-II

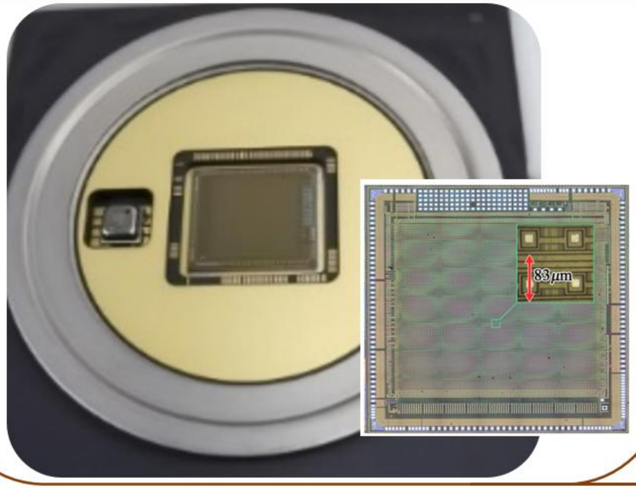

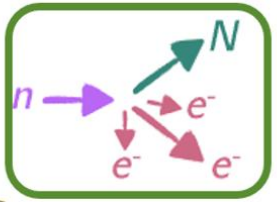

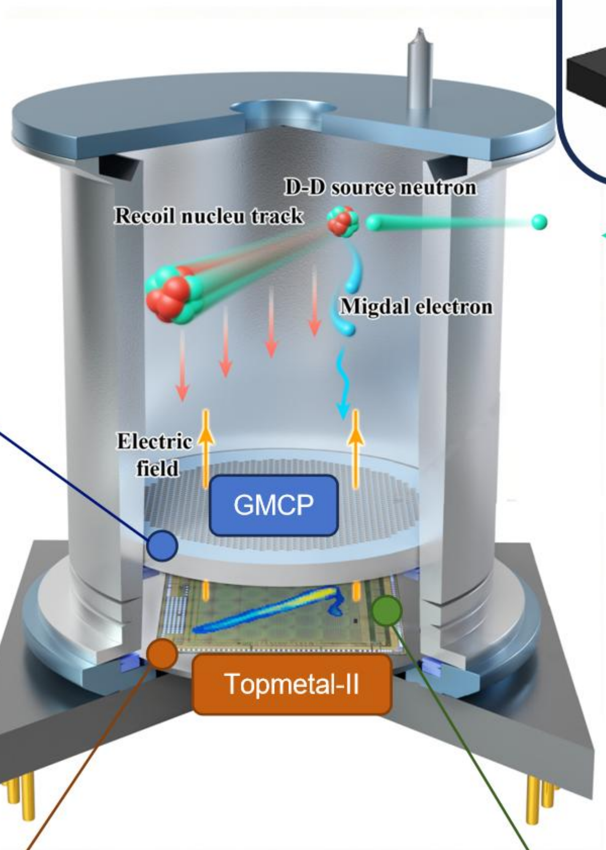

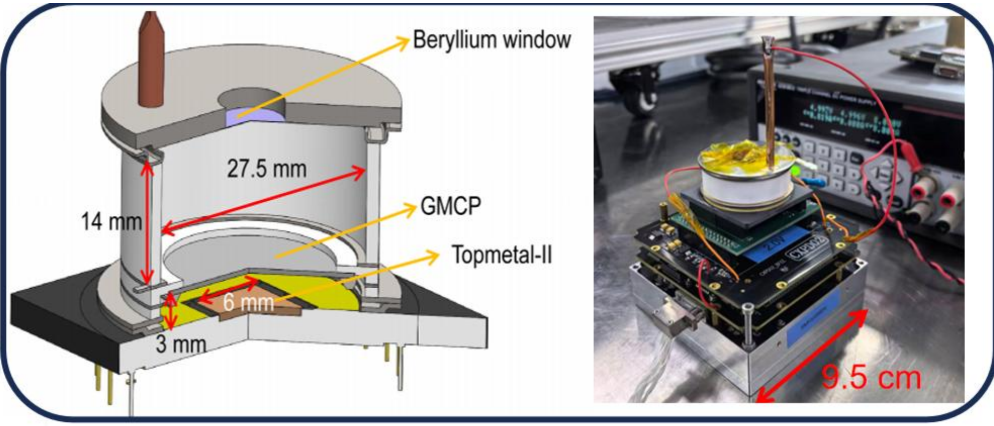

Migdal topology

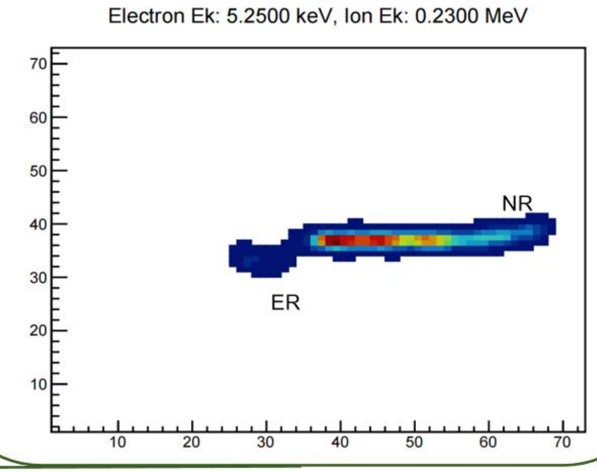

Development of the detector design

10.1088/1748-0221/13/06/P06011

2015-2018

THGEM/Mesh+CCD

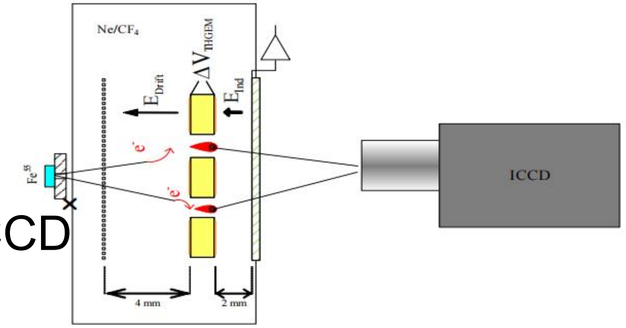

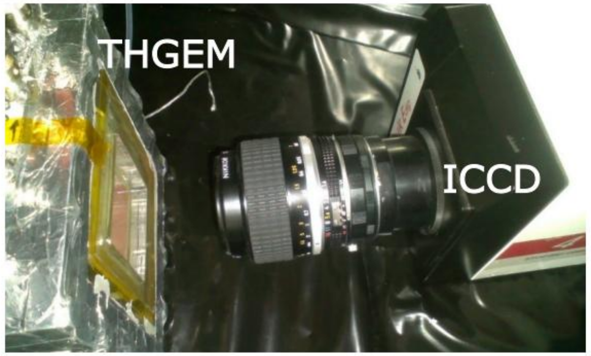

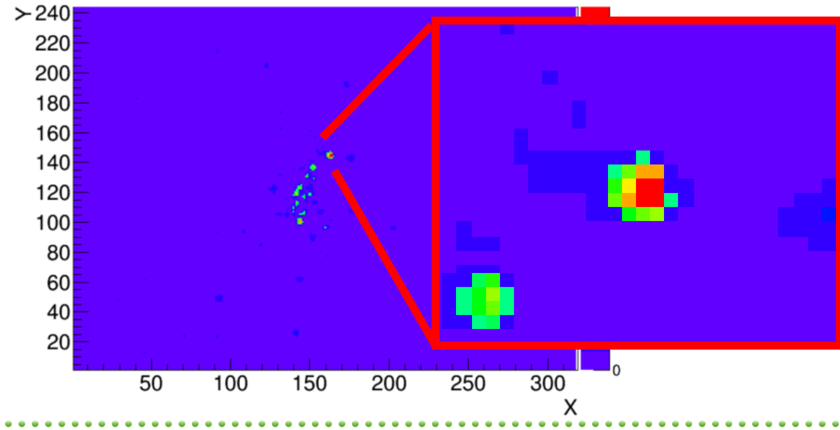

2019-2020

THGEM+Topmetal

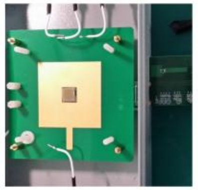

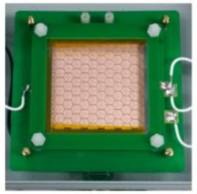

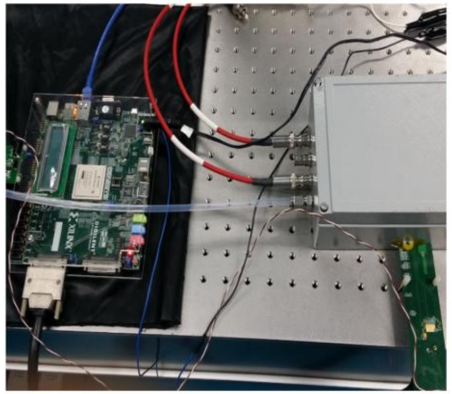

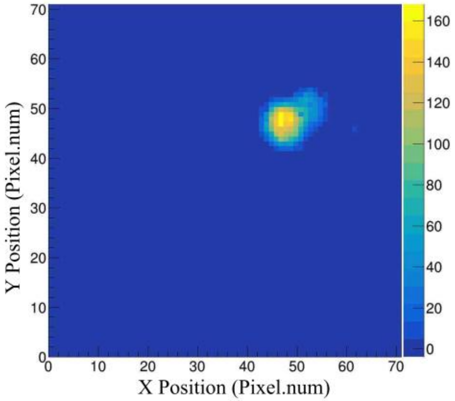

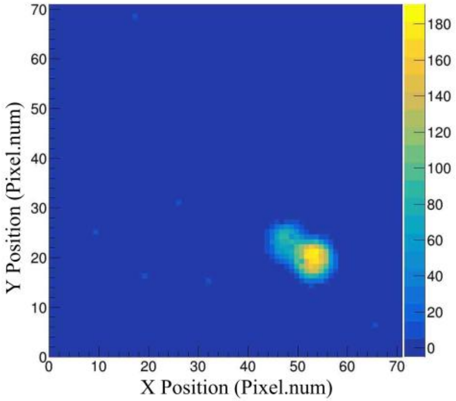

2021-now
GMCP+Topmetal

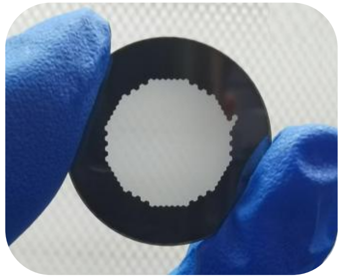

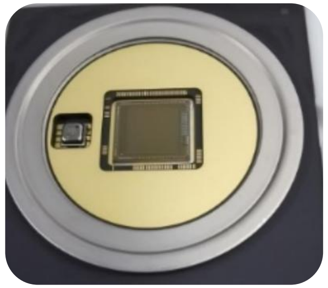

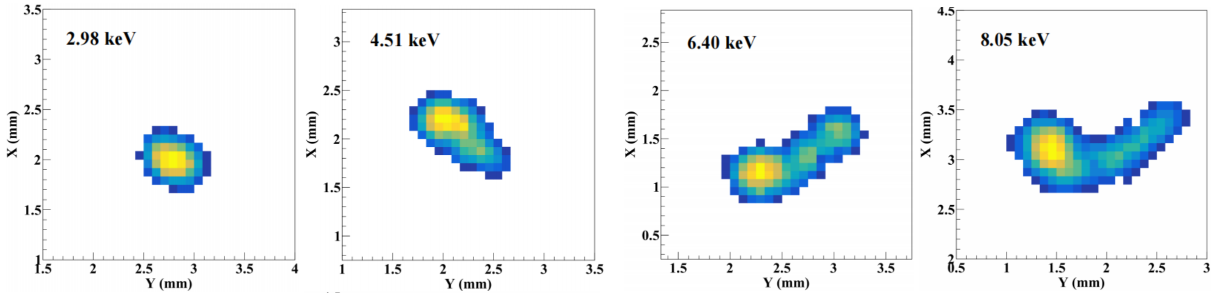

Detector Requirements

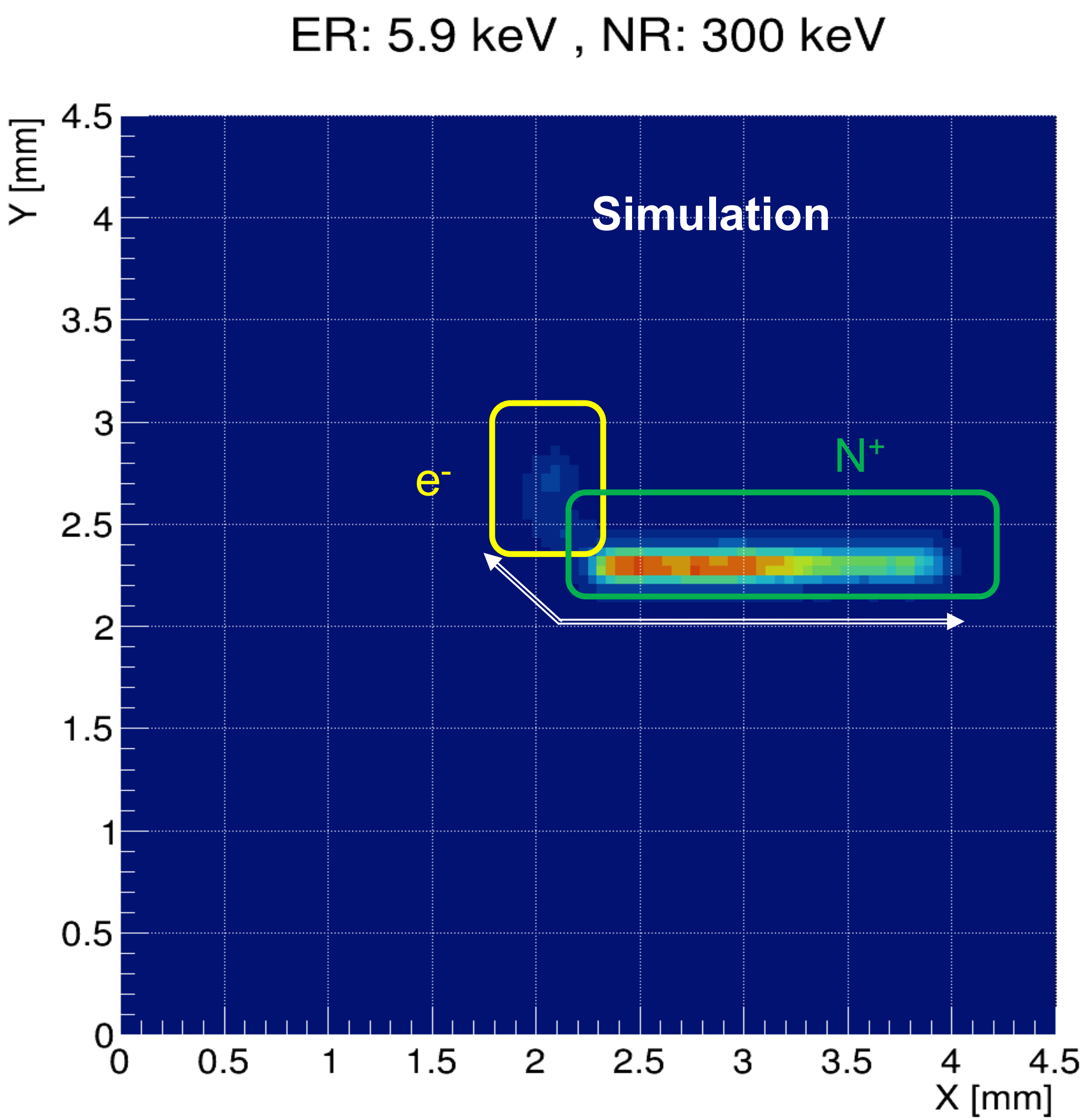

- **ER~keV, NR~hundreds keV**
  - Good energy resolution
  - Large dynamic range.
- **ER shares vertex with NR**
  - Good vertex resolution
- **Reduce possible background**
  - Good time resolution

Performance Stability

- low leakage rate and material degassing rate specifications
- Suppress the charge accumulation effect

Bulk Resistance

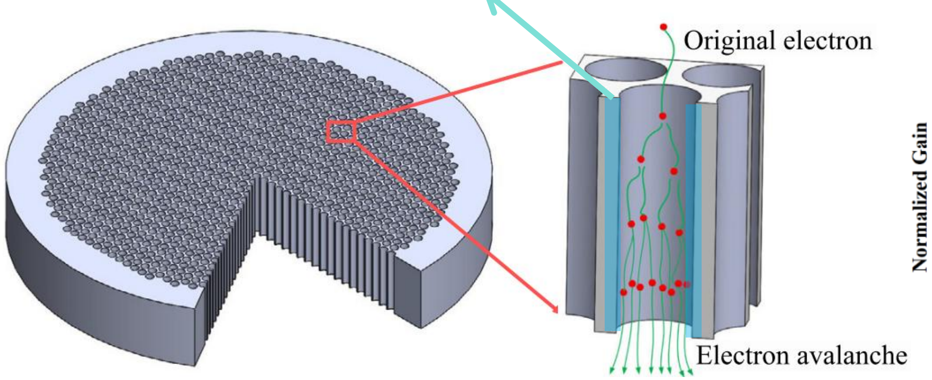

10.1016/j.nima.2023.168499

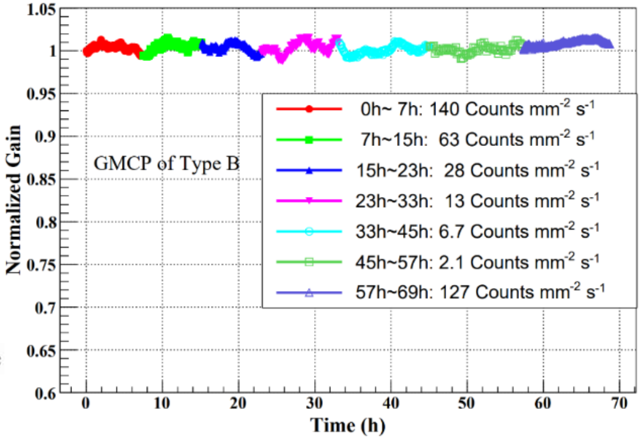

stability at different counting rates

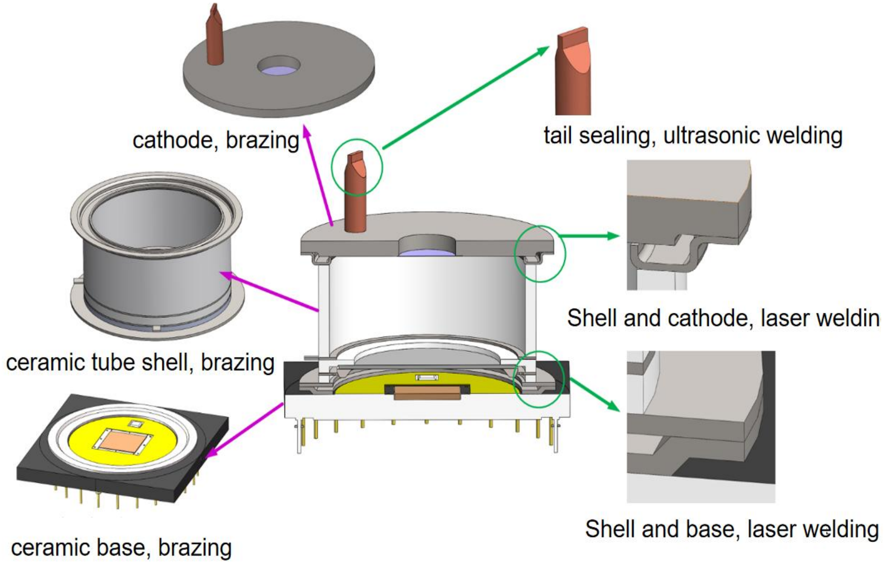

	Type A	Type B	Type C	Type D	Type E
Hole diameter	50 μm	50 μm	50 μm	60 μm	30 μm
Thickness	400 μm	400 μm	300 μm	300 μm	300 μm
Hole pitch	60 μm	60 μm	60 μm	80 μm	40 μm
GMCP resistance	∞	5 GΩ	3 GΩ	5 GΩ	∞
Hydrogen reduction	Without	With	With	With	Without

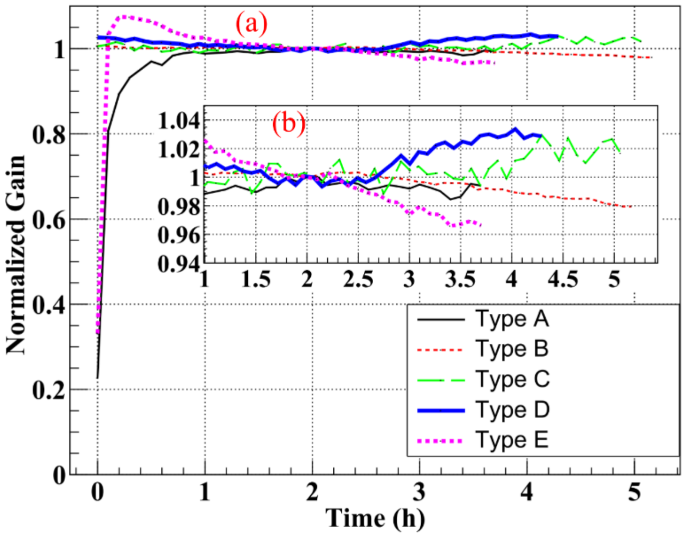

Leak rate: ~7.6^{-11} Torr·L/s

GMCP Development – Hydrogen Reduction tech for Preparing Bulk Resistance to Eliminate Charge Accumulation

Optimize the spatial resolution

various gas mixtures:
$He/Ar/Kr/Xe+CO_2/CH_4/i\text{-}C_4H_{10}/DME(C_2H_6O)/CF_4$

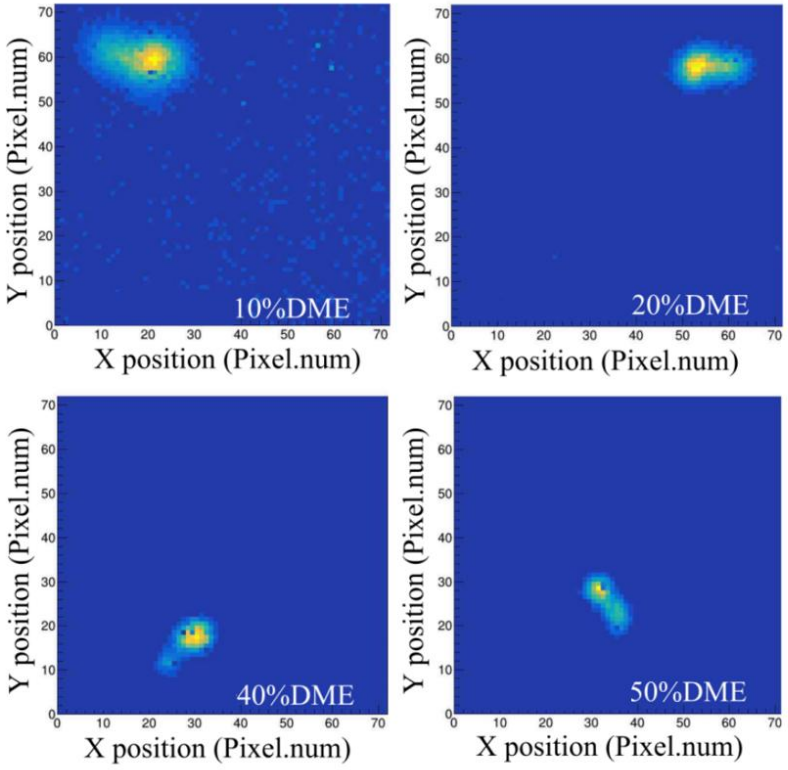

Parameter testing for various gases and gas mixtures

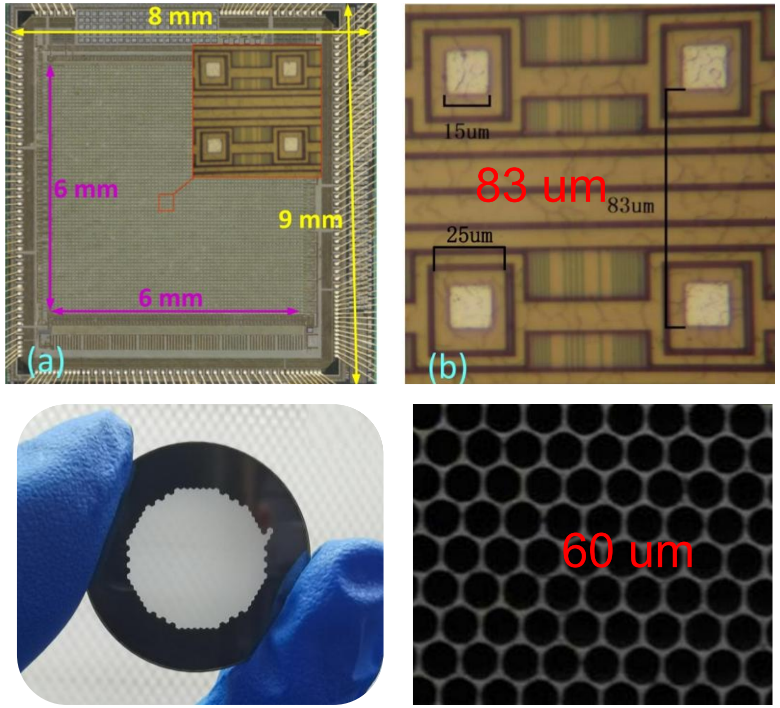

high-granularity device

10.1007/s41365-021-00903-0

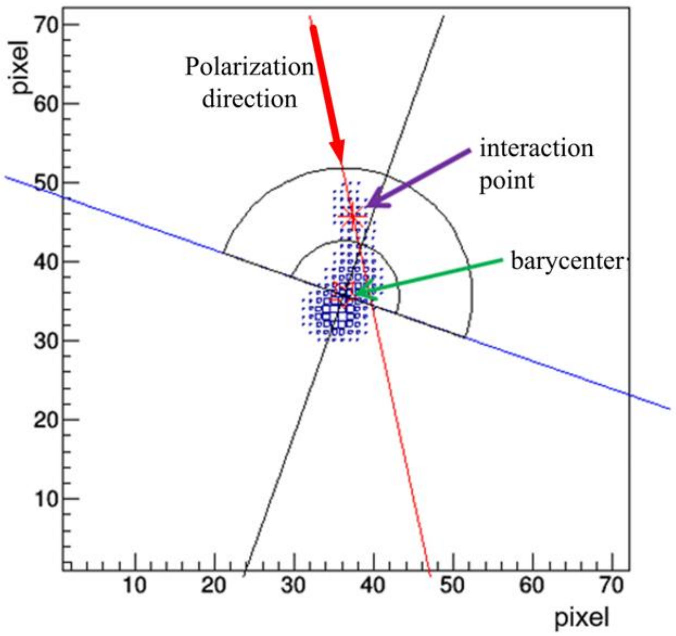

adaptive cutting
vertex reconstruction

Energy calibration

Energy (keV)	Crystal	Incident radiation	Diffraction angle(deg)
2.98	Si(111)	Ag L_α	41.6
4.51	Si(220)	Ti K_α	45.8
5.40	Si(311)	Cr K_α	44.5
6.40	Si(400)	Fe K_α	45.5
8.05	Si(224)	Cu K_α	44.1

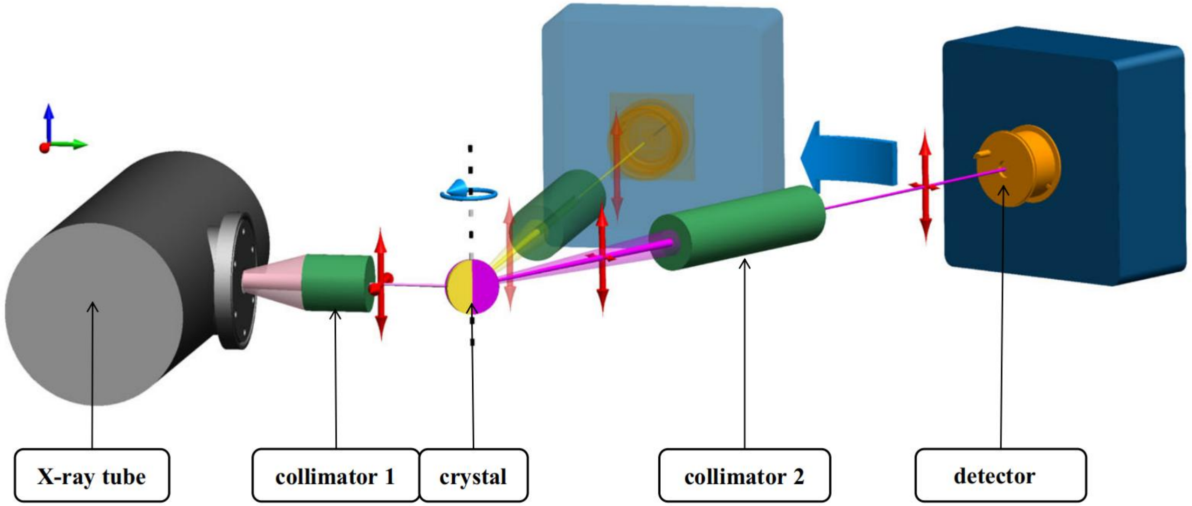

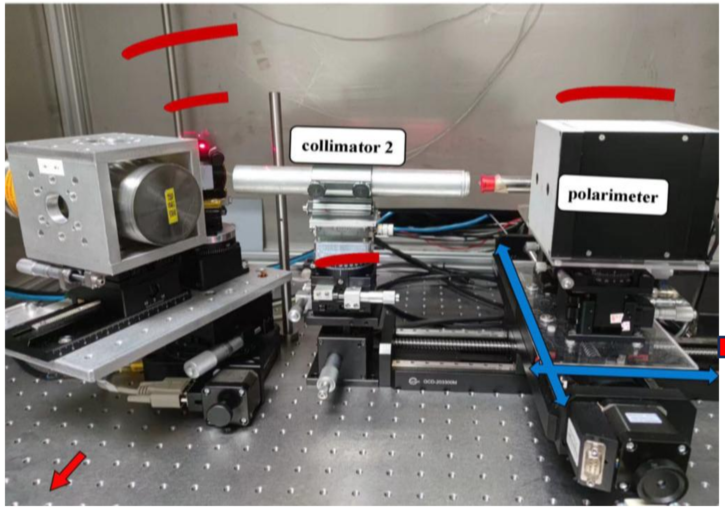

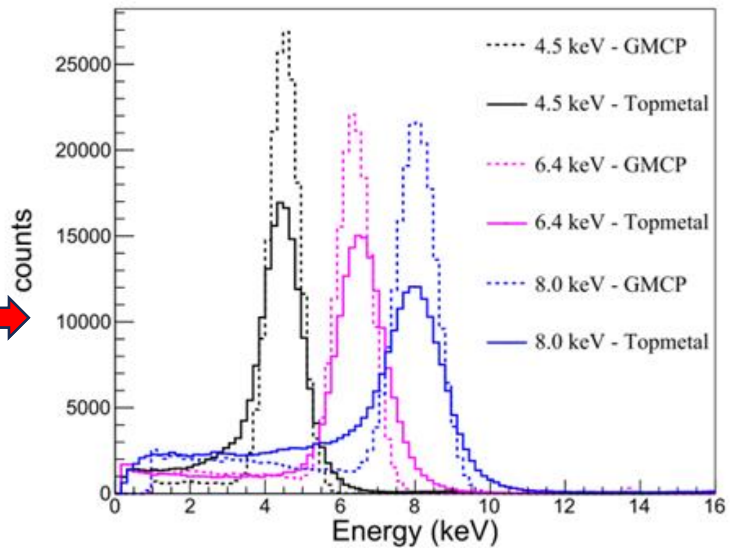

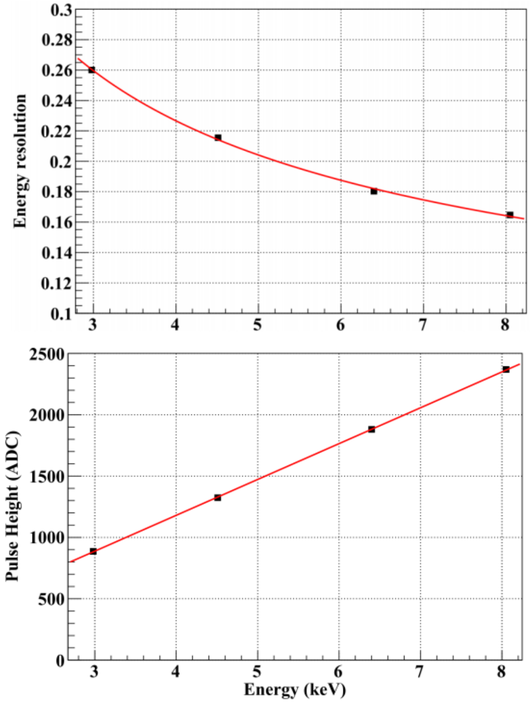

$\propto 1/\sqrt{E}$

10.1007/s10686-023-09905-9

monoenergetic X-ray platform

Vertex resolution

copper plate

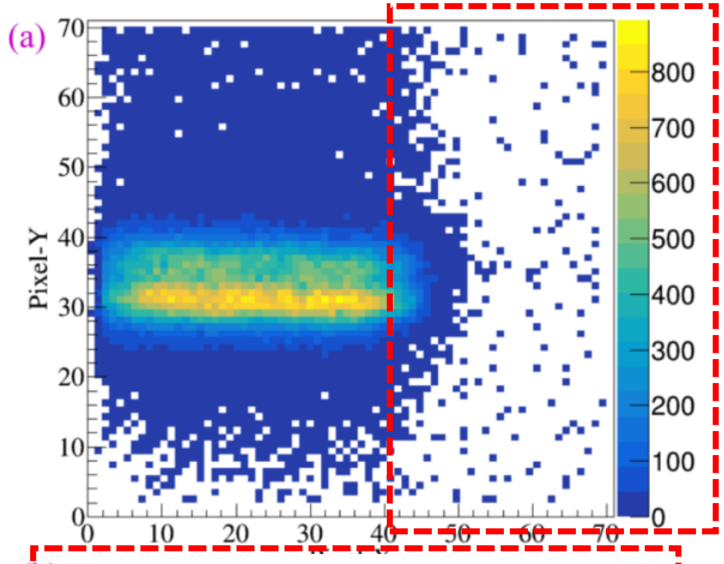

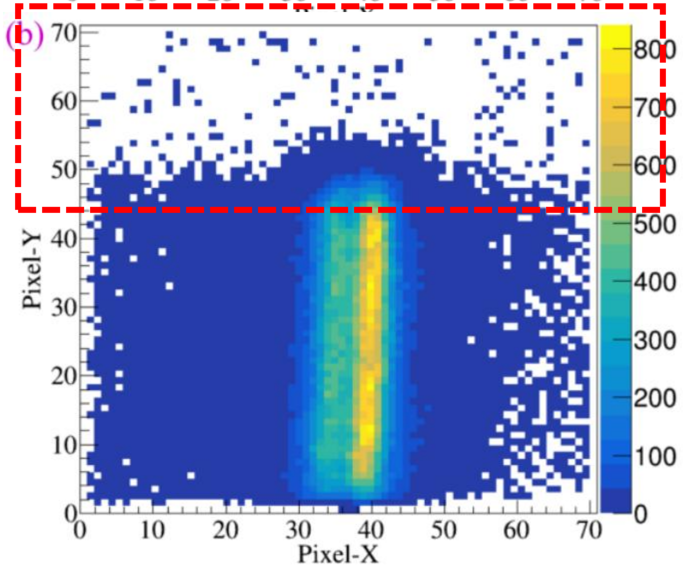

6.4 keV X-ray imaging with half the area shielded by a copper plate

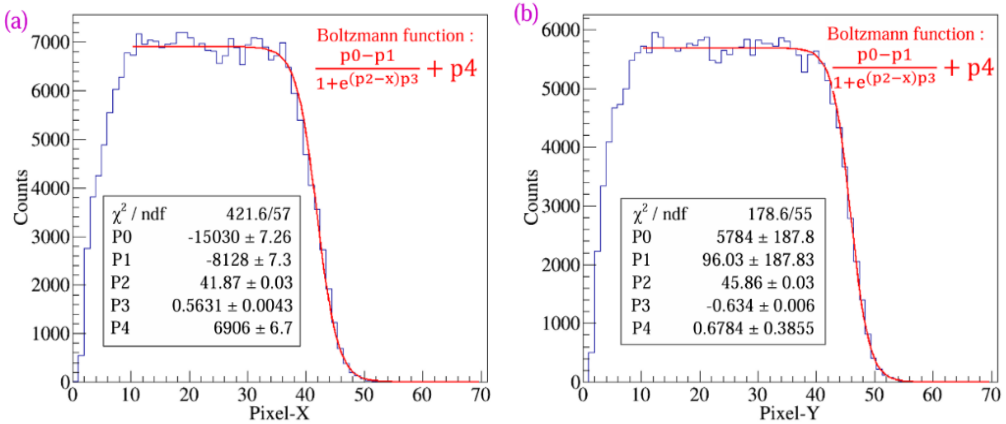

reconstruct the vertices of p.e. tracks

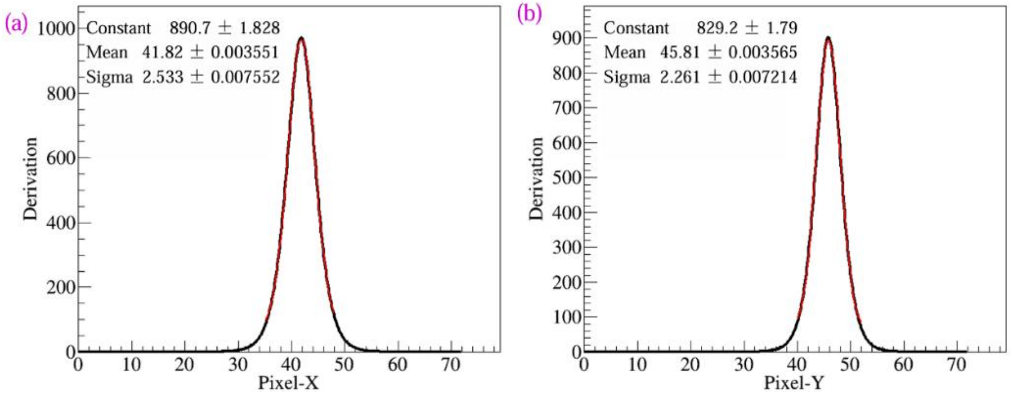

position resolution @ 6.4 keV

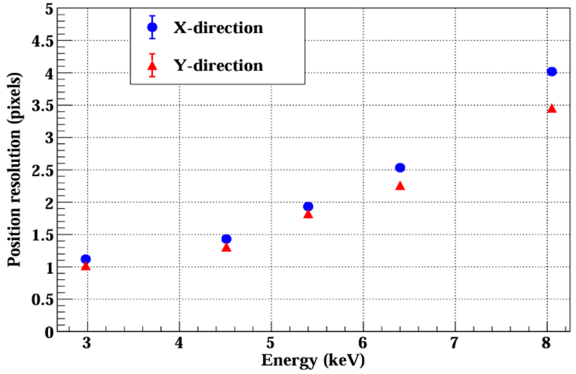

position resolution at different energies

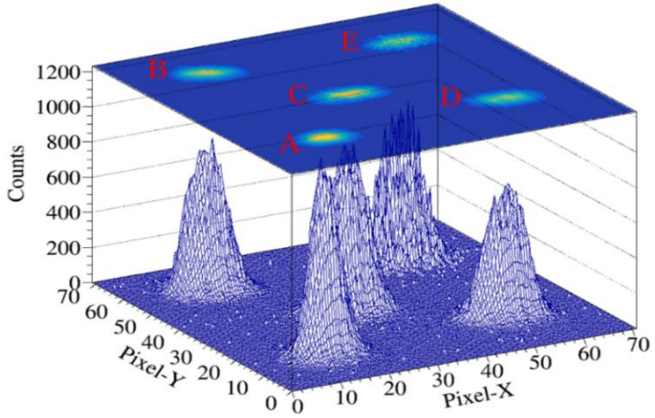

spatial resolution at different positions

[10.1088/1748-0221/19/04/P04039](https://doi.org/10.1088/1748-0221/19/04/P04039)

Time resolution

GMCP trigger : 100 Mhz (10 ns)

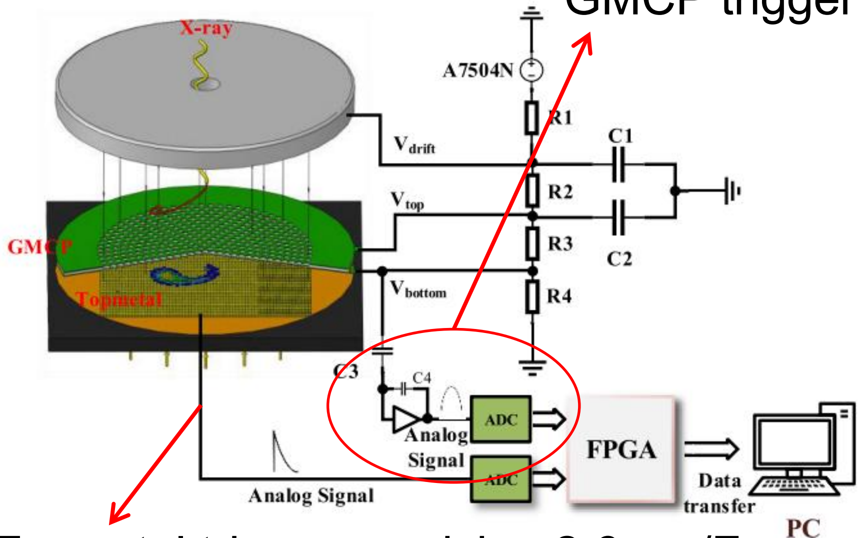

Topmetal trigger precision:2.6 ms/Frame

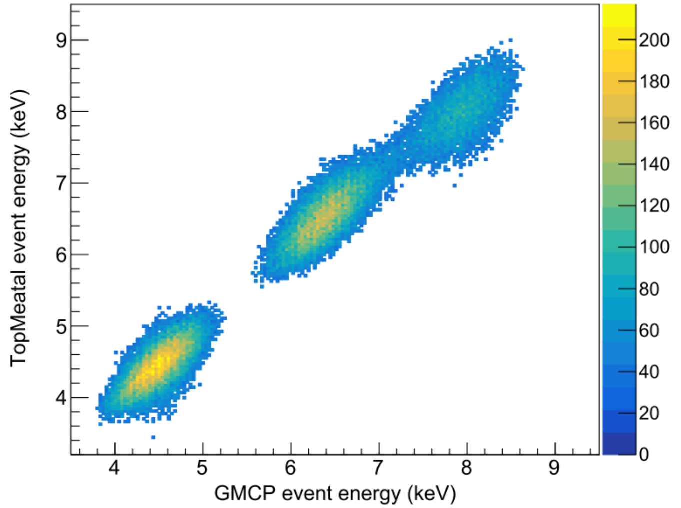

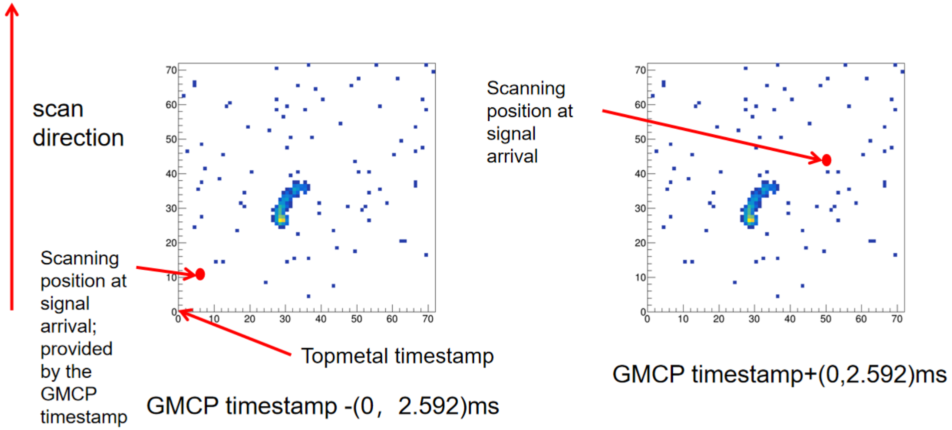

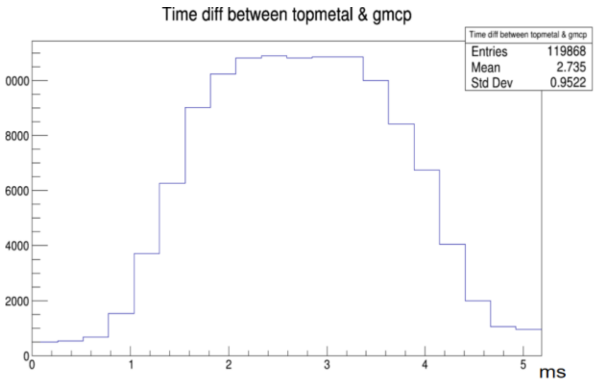

6 ms Timewindow

IEEE Trans. Nucl. Sci., 70, 1288-1295

deltaT = $t_{topmetal}$-t_{GMCP}+Pixel_order*500ns

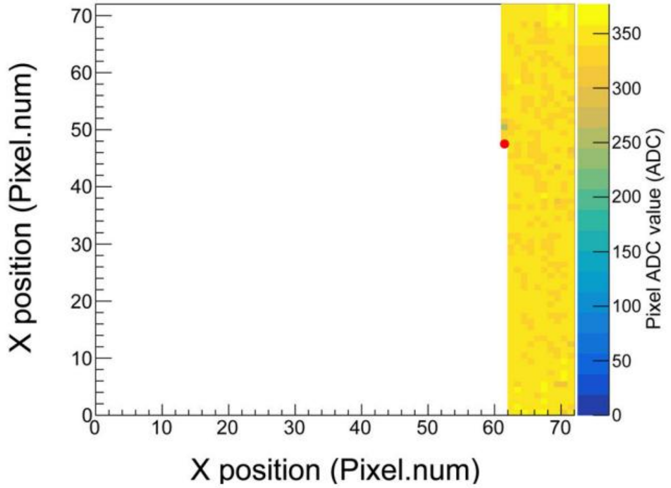

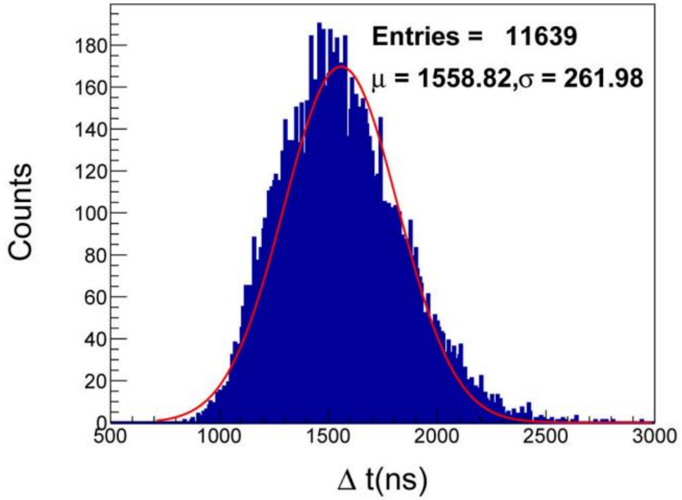

time resolution test results

Detector performance

Energy resolution

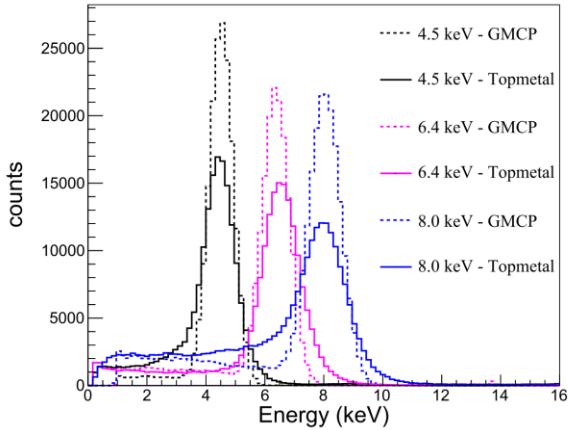

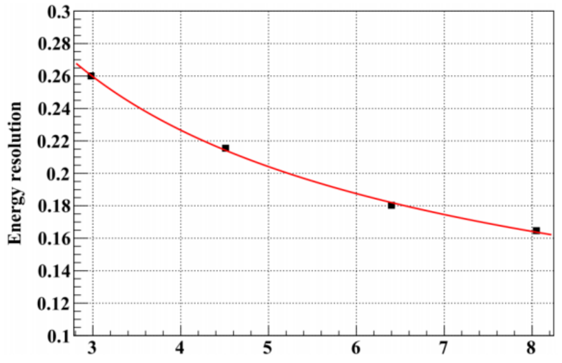

- Good linear energy response
- 20%-30% energy resolution(FWHM)
- Energy resolution follows the relationship ~ $1/\sqrt{E}$

Dynamic range

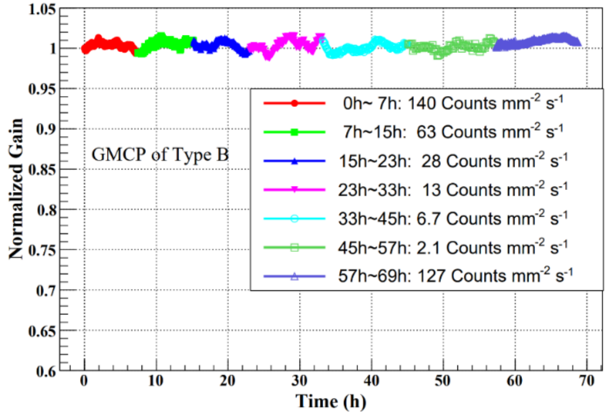

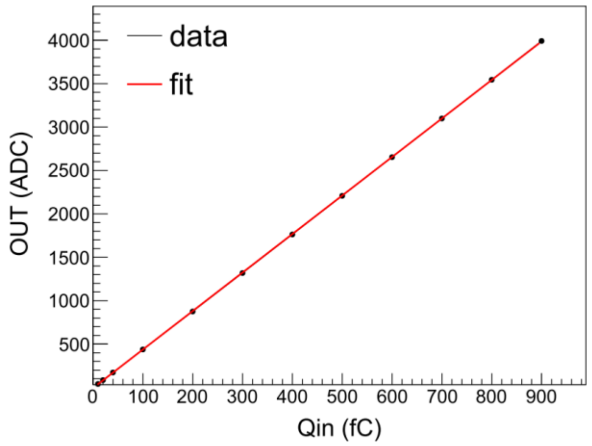

- Stable gain under different count rates(no pile up)
- Good linearity in charge response

Vertex resolution

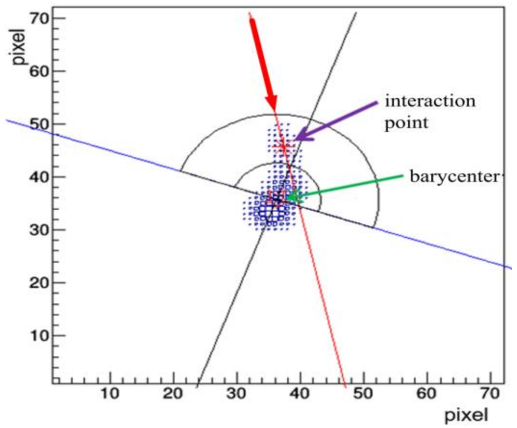

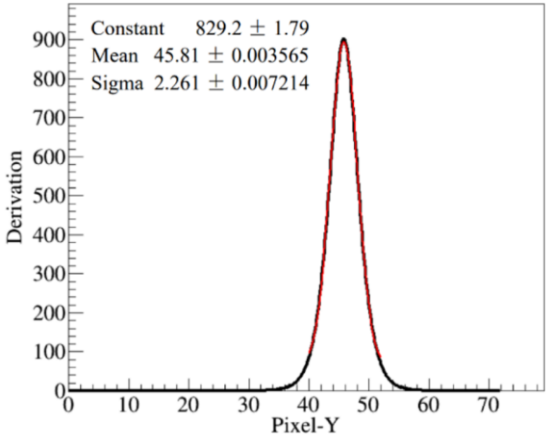

- ~200 μm vertex resolution @ 6.4 keV

Time resolution

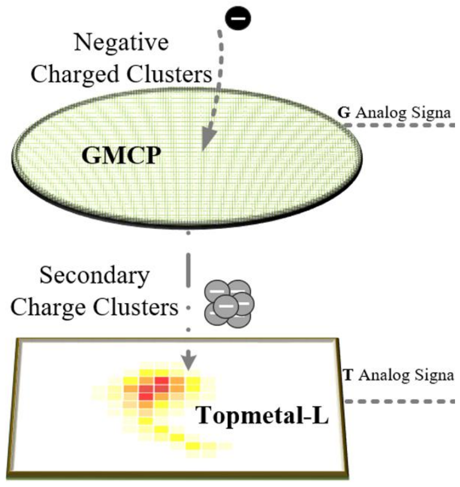

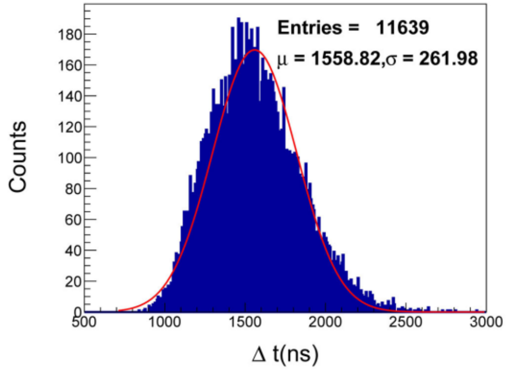

- ~262 ns time resolution

Simulation framework

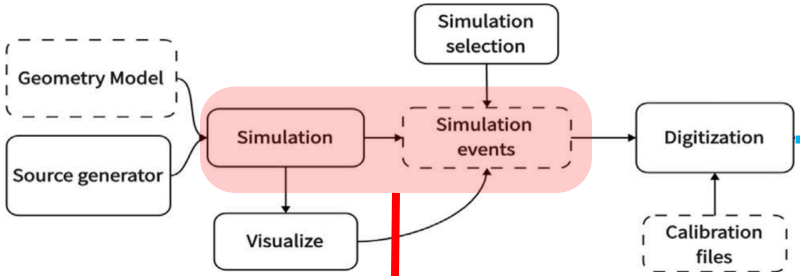

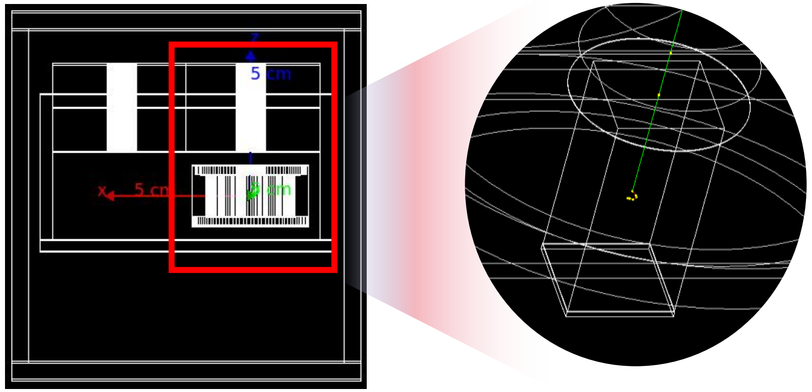

- ✓ Simulate Migdal effect interaction with detector
- ➢ Simulate different interaction
- ➢ Provide energy deposit

https://github.com/ElsevierSoftwareX/SOFTX-D-23-00679

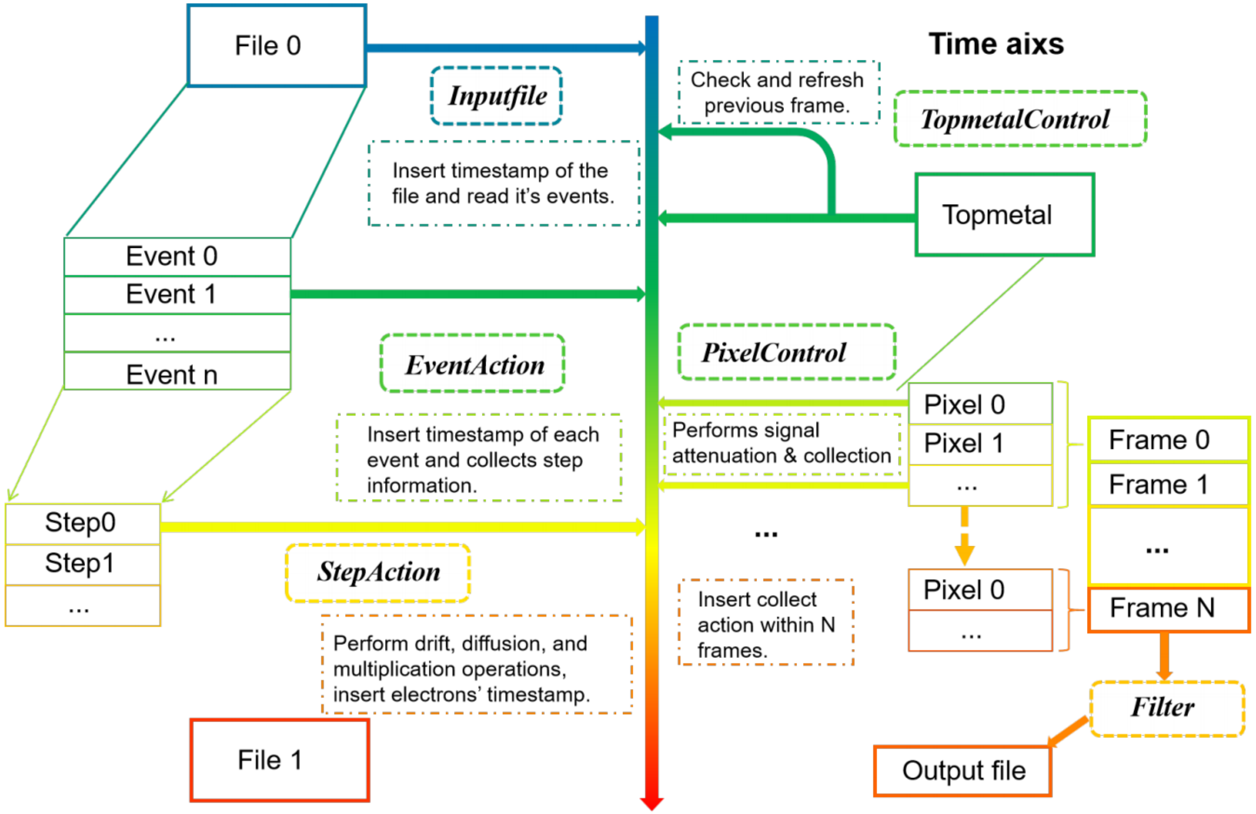

- ✓ Analog detector digital readout
- ➢ Simulate electron drifts, multiplies, collected procession
- ➢ Output file for data analysis and reconstruction algorithm

Comparison of experimental/simulation results

6.4 keV photo-electron

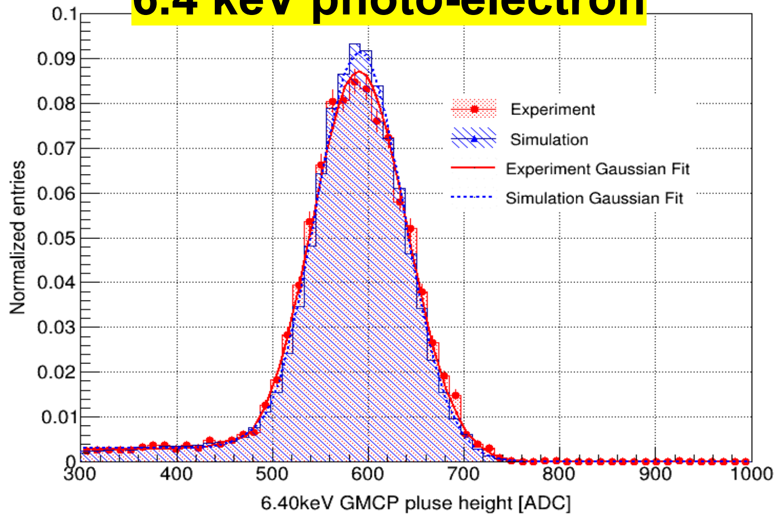

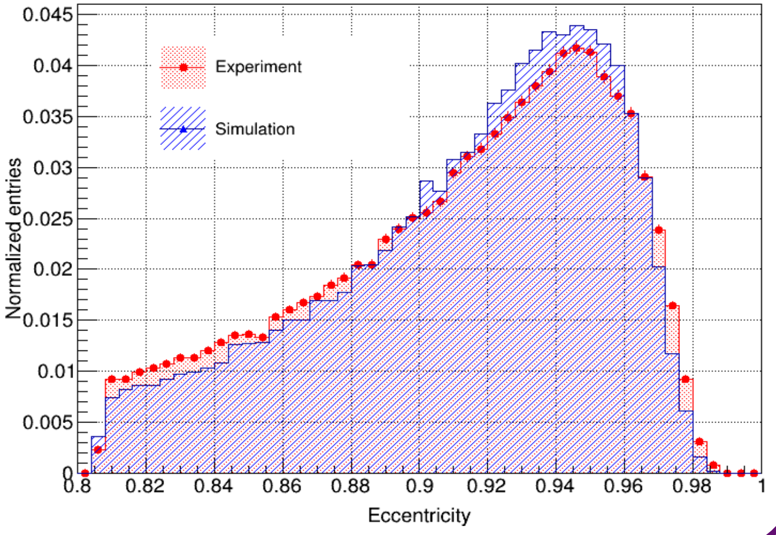

^{241}Am alpha source

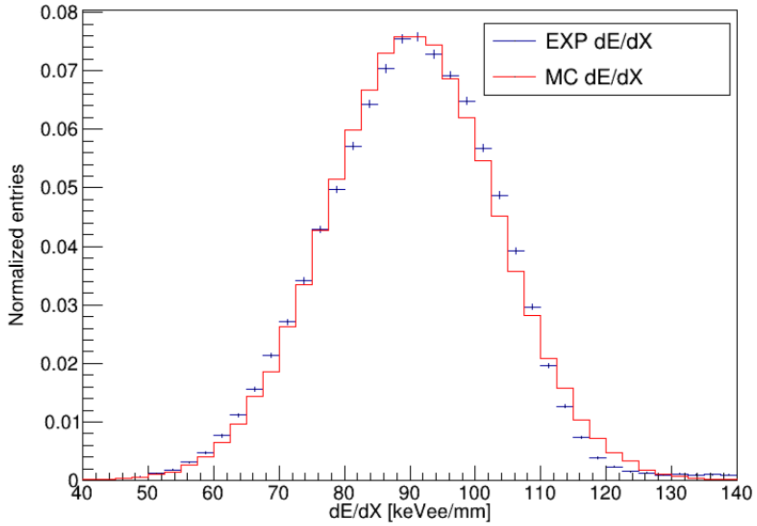

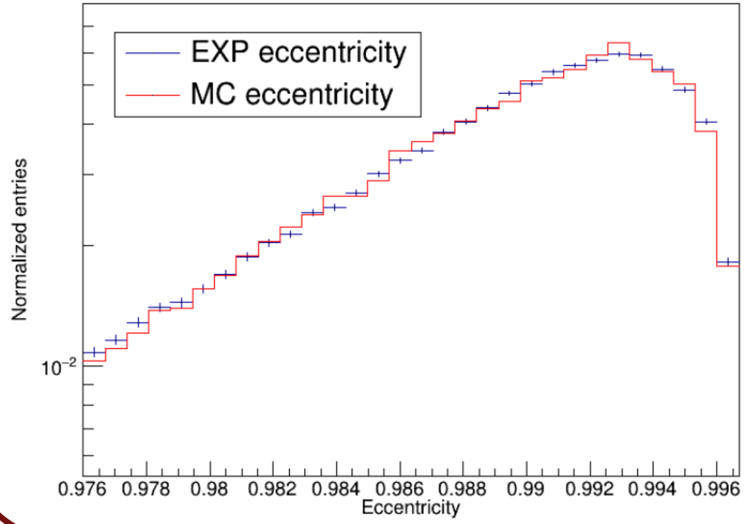

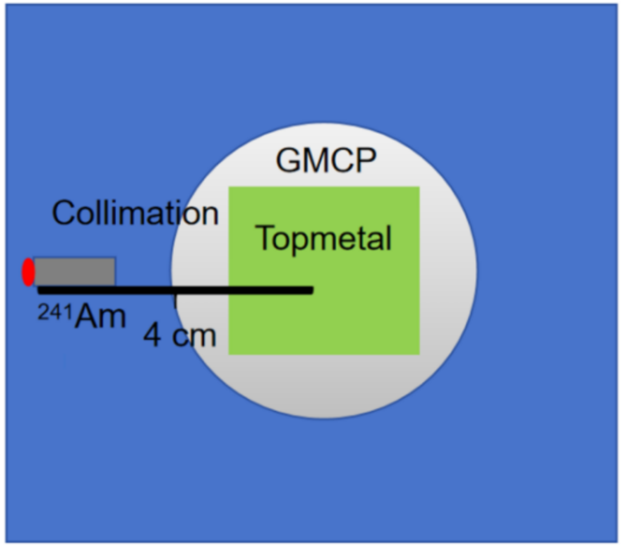

Top view

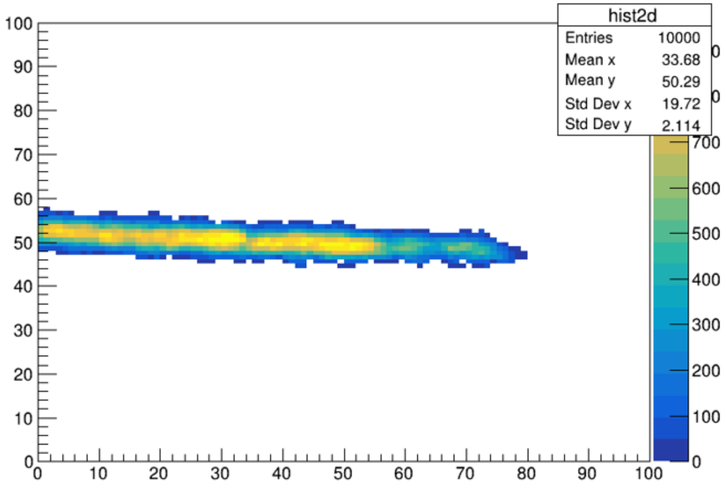

MARVEL Experiment

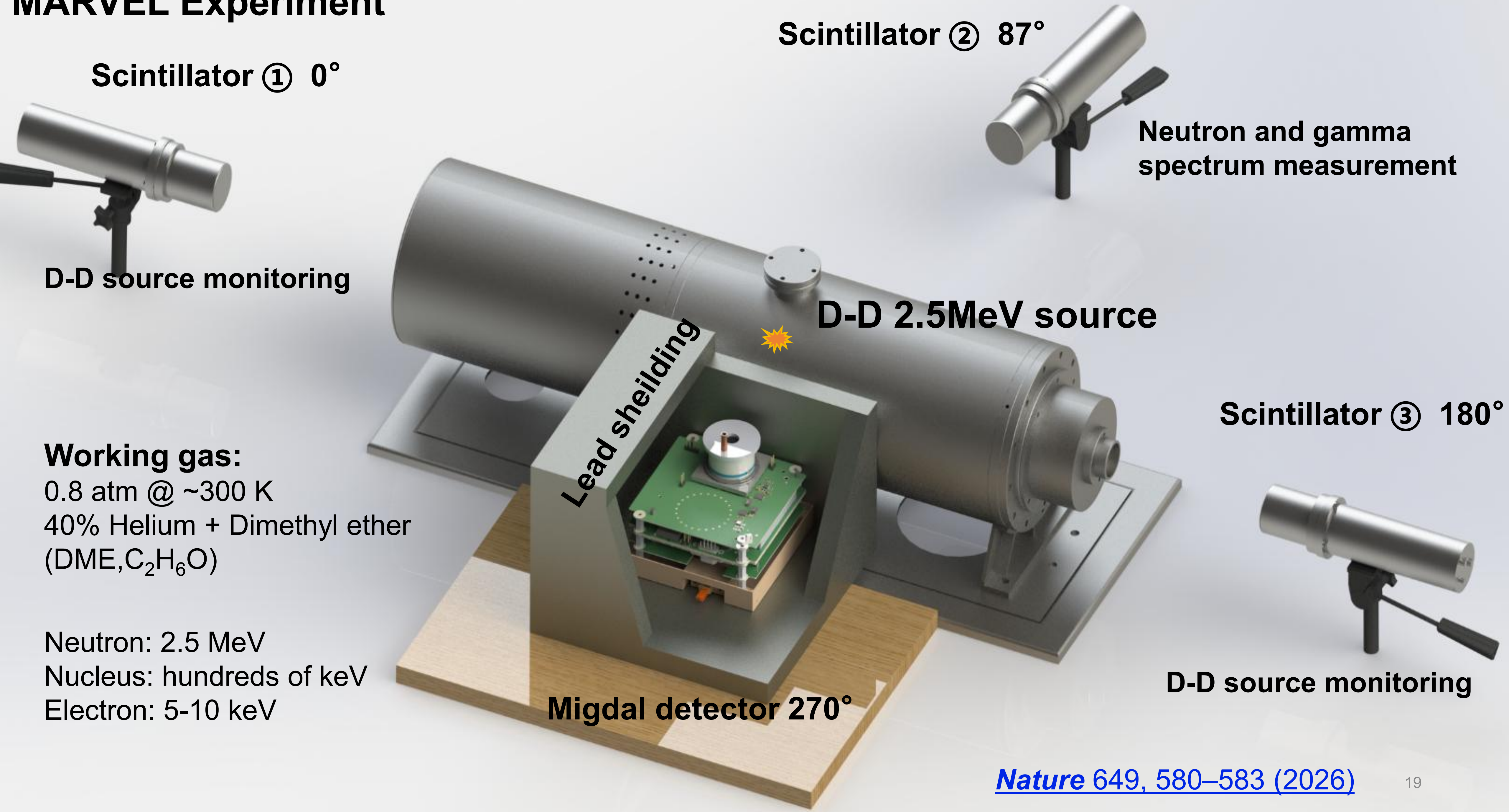

Working gas:
0.8 atm @ ~300 K
40% Helium + Dimethyl ether (DME, C_2H_6O)

Neutron: 2.5 MeV
Nucleus: hundreds of keV
Electron: 5-10 keV

Nature 649, 580–583 (2026)

Data taking

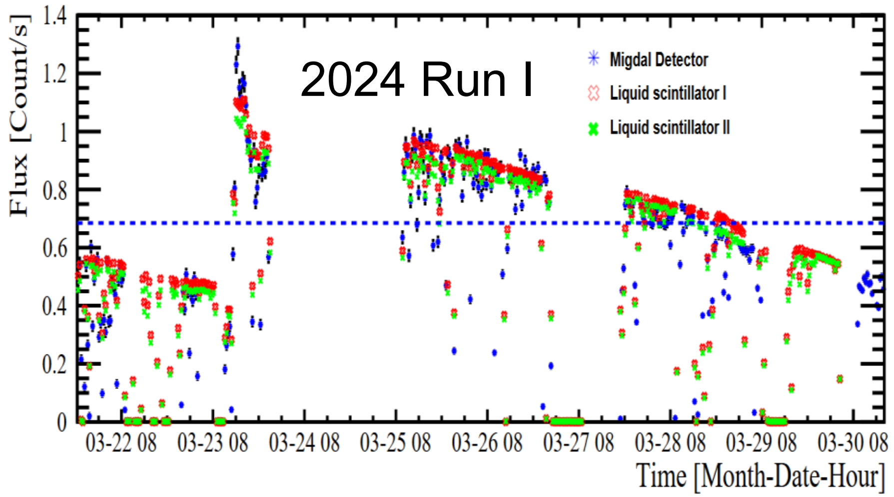

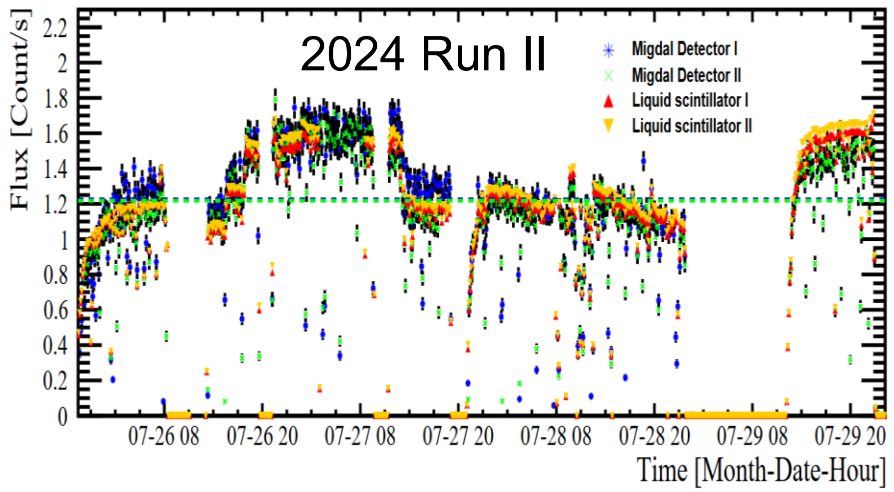

Flux

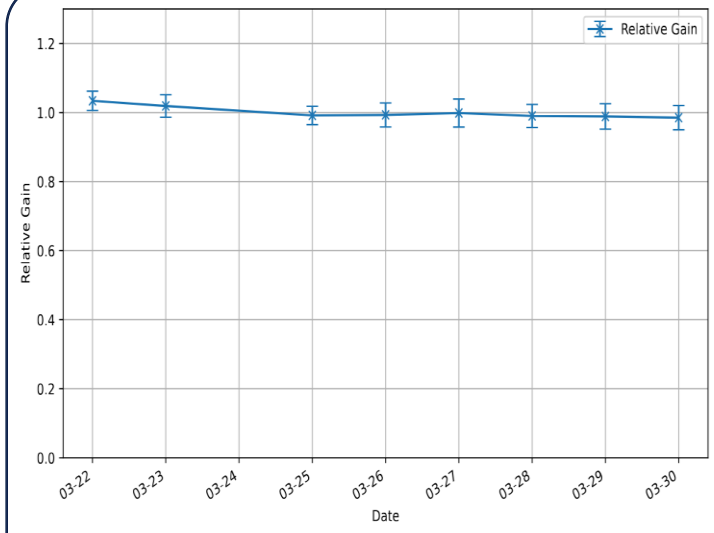

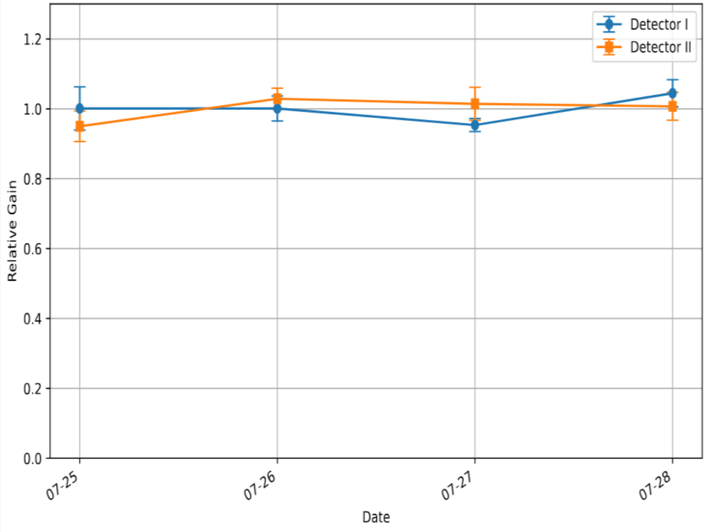

Gain

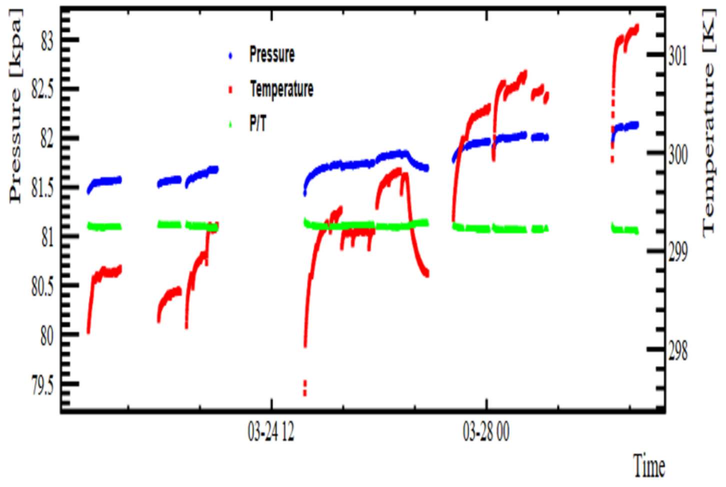

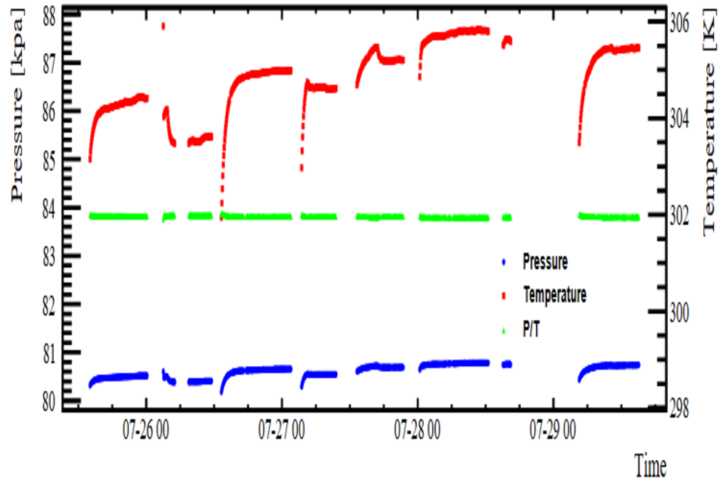

Pressure & temperature

AI-assisted event selection

Data → YOLO*1 preselection → NR reconstruction → ER reconstruction → Vertex cut

Inspired by MIGDAL collaboration's work: 10.1103/PhysRevD.111.072004

YOLOv8.2

Labeling

Dataset		Train	Valid
Exp	^{55}Fe	3000	1493
	D-D	2994	1354
Sim	ER	1200	301
	NR	1200	301
Total		8394	3449

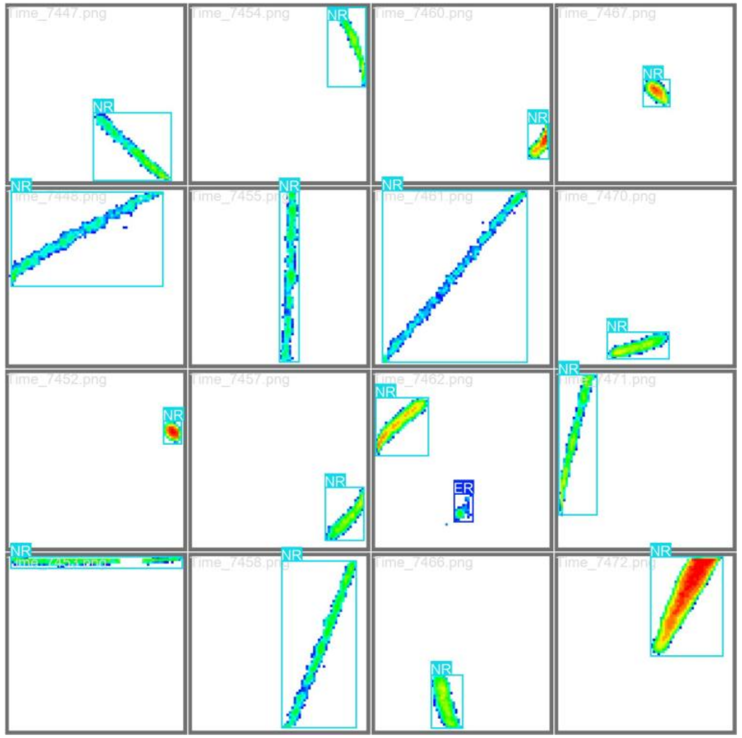

Training

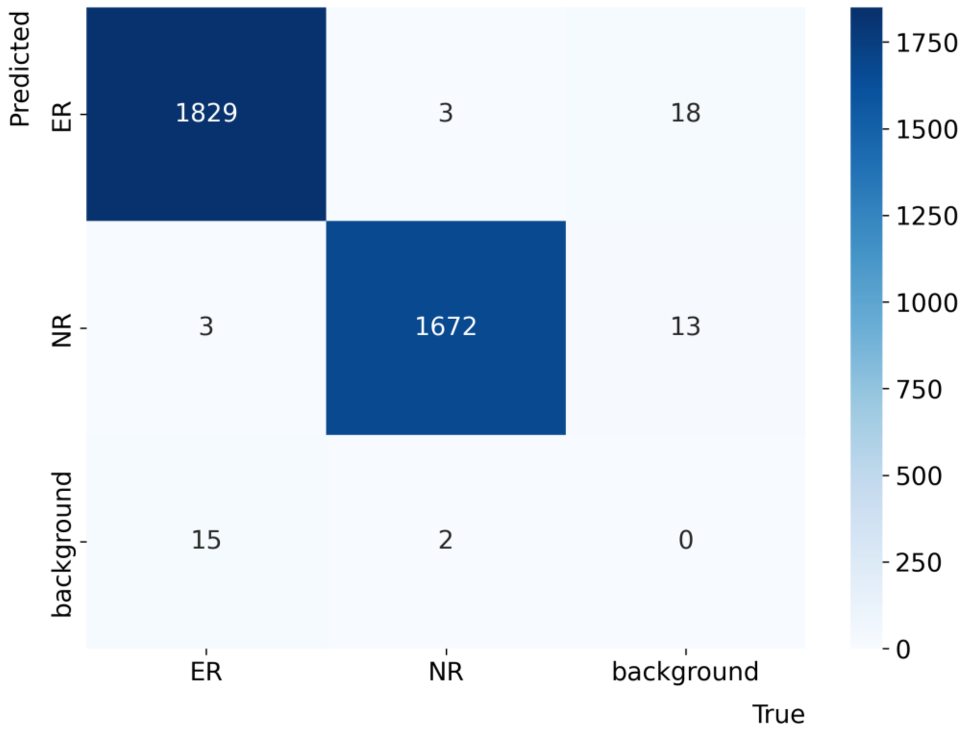

*1 https://github.com/ultralytics/ultralytics

AI-assisted event selection

Data → YOLO*[1] preselection → NR reconstruction → ER reconstruction → Vertex cut

1. Search for the NR vertex through recursive iteration:

$$(x_0,y_0) \xrightarrow{\mathrm{ADC}\cdot exp\,(d/d_0)} (x_n,y_n)$$

2. Fit the NR(direction, diffusion σ) and remove it from the image.

3. Search for the electron vertex using adaptive cutting algorithm.

4. Determine whether the electron vertex is adjacent to the nucleon vertex.

$$R = \frac{D - 4\sigma}{L_{\mathrm{ER}}} < 0.5$$

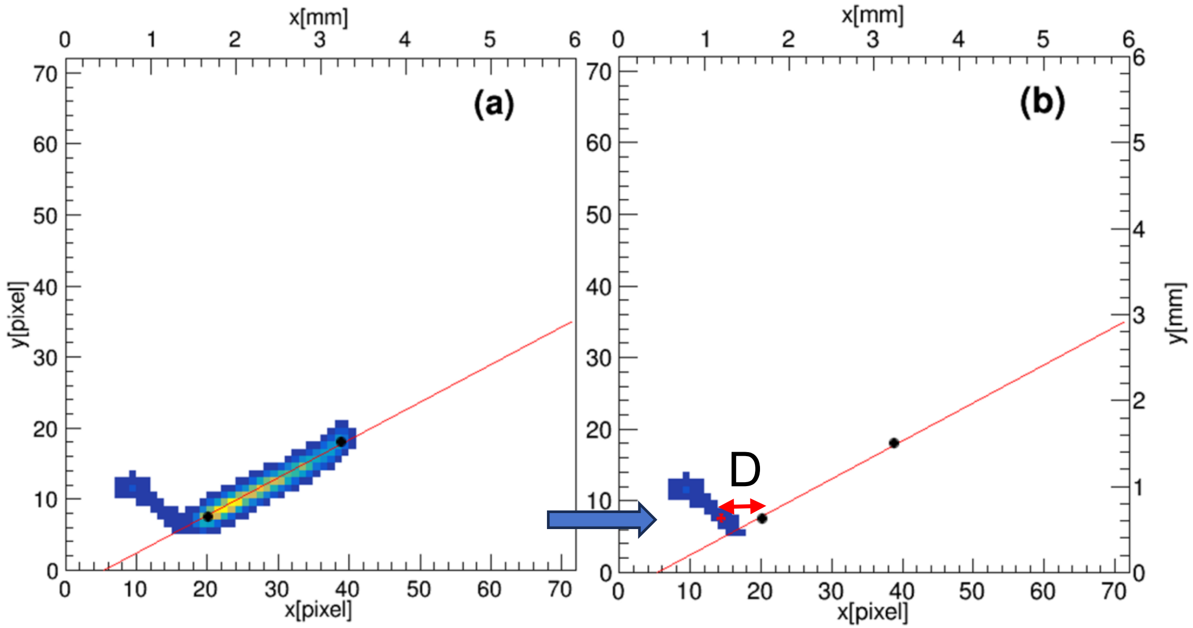

Migdal candidates

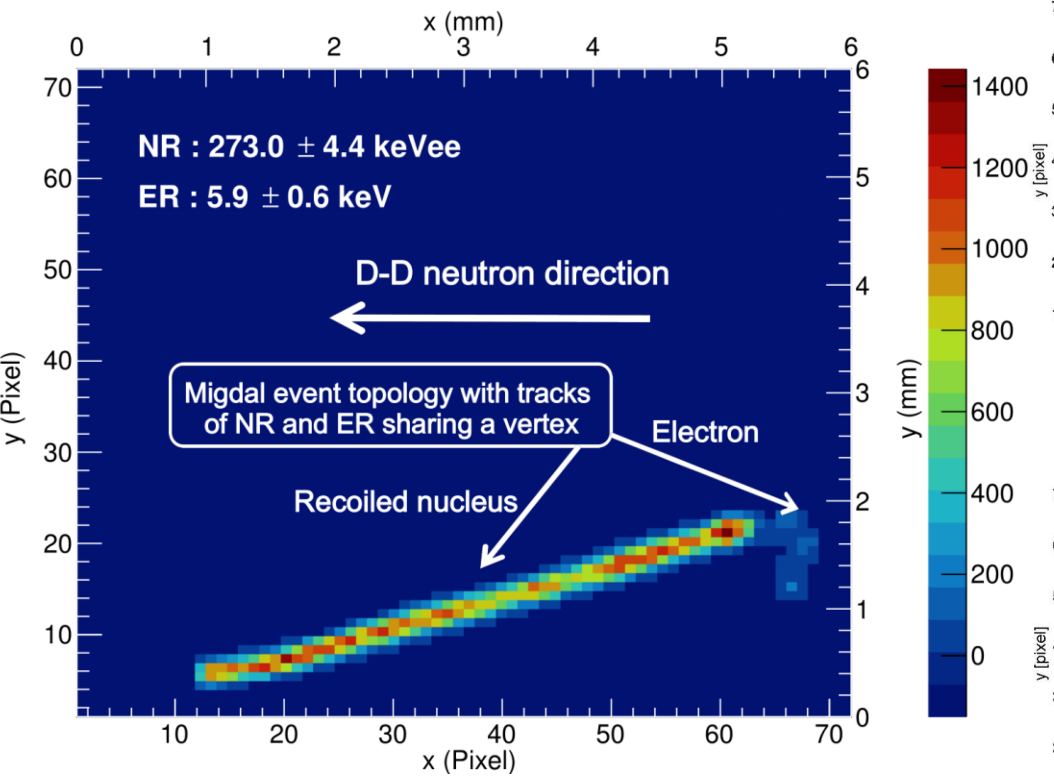

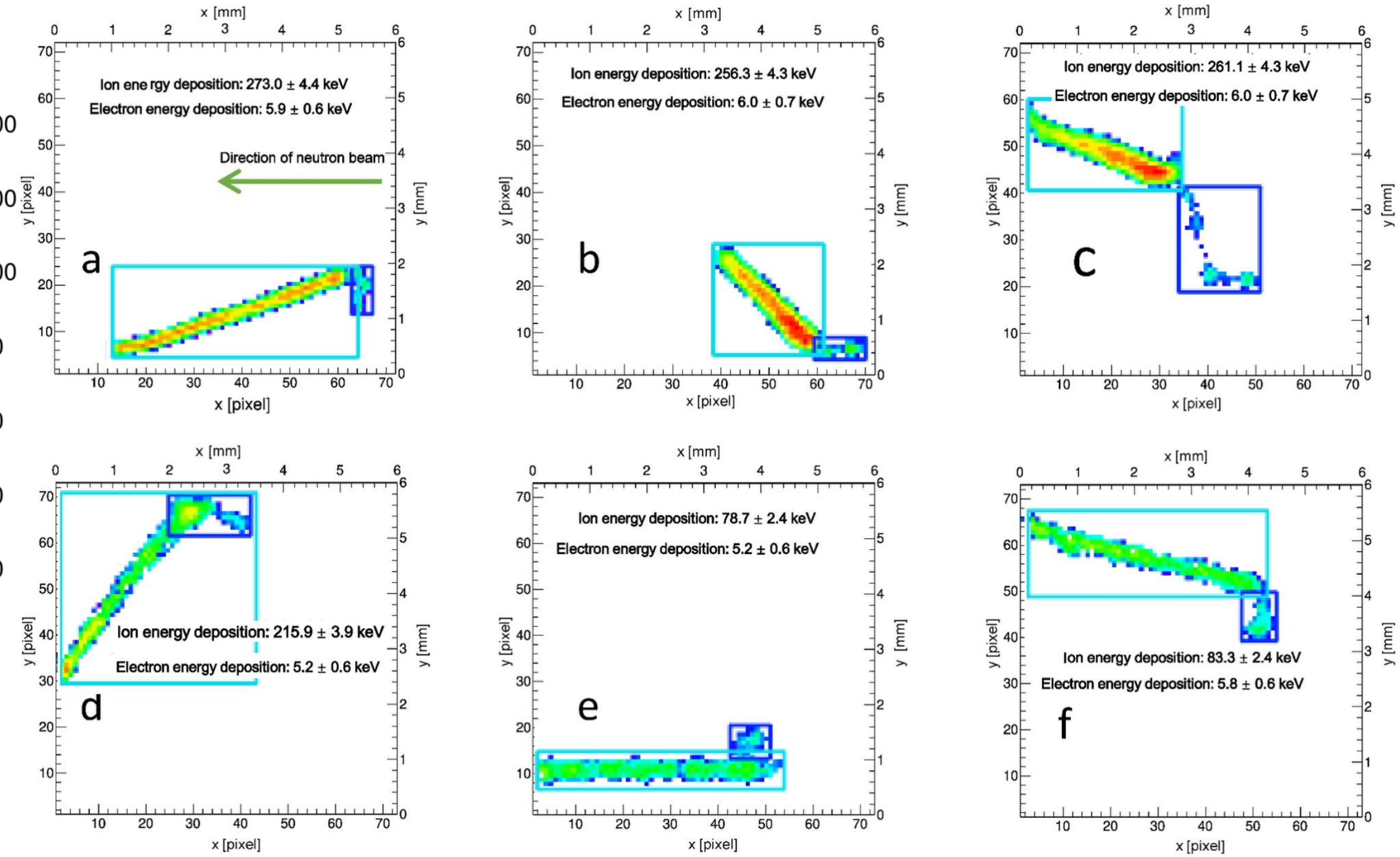

Characteristic distribution of ERs and NRs

$$5\ keV_{ee} < Ee < 10\ keV_{ee}, E_{nr} > 35keV_{ee}$$

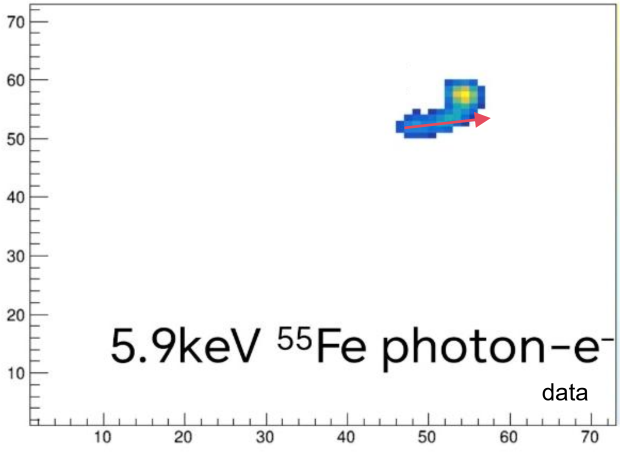

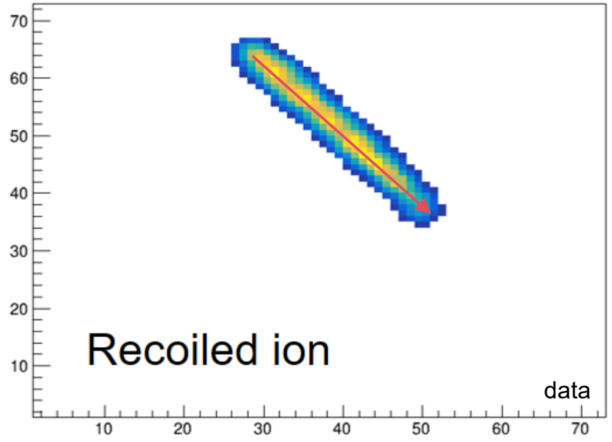

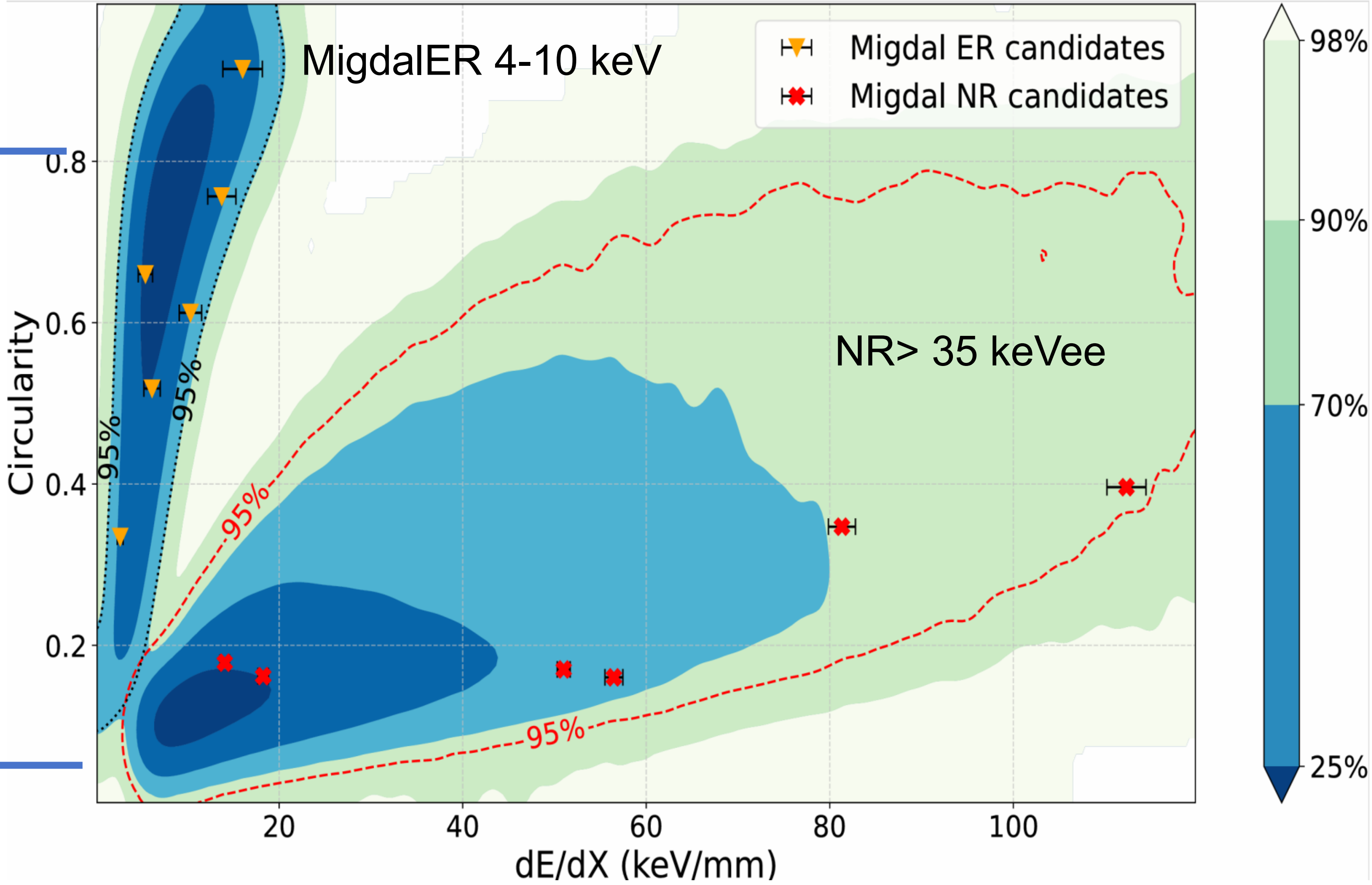

Background

Background Component	Description	Expectation value (5 - 10 keV)	Method
Recoil induced δ ray	δ electron near NR track origin	0.035 ± 0.023(stat.) ± 0.0068(sys.)	Data driven
Particle Induced X-ray Emission			
X-ray emission	Photoelectron near NR track origin	0	
Auger electrons	Auger electron near NR track origin	0	
Bremsstrahlung processes			
Quasi-Free Electron (QFEB)	Photoelectron near NR track origin	≈ 0	
Secondary Electron (SEB)	Photoelectron near NR track origin	≈ 0	
Atomic (AB)	Photoelectron near NR track origin	≈ 0	
Nuclear (NB)	Photoelectron near NR track origin	≈ 0	
Random track coincidences	Photo-/Compton electron near NR track	0.180 ± 0.022(stat.) ± 0.042(sys.)	Data driven
Muon induced δ ray	δ electron near NR track origin	0.013	MC+Data
Gas radioactivity			
Trace contaminants	Electron from decay near NR track origin	0.001 ± 0.00087(sys.)	Data driven
Neutron activation	Electron from decay near NR track origin	≈ 0	
Secondary nuclear recoil fork	NR track fork near track origin	≈ 0	
Total background		0.229 ± 0.032(stat.) ± 0.043(sys.)	

Recoil induced δ electron

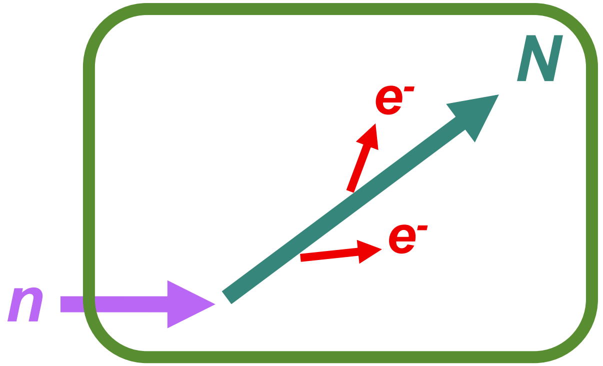

$$E_\delta[\text{keV}] = \frac{8.715}{(1+A)^2} E_n[\text{MeV}]$$

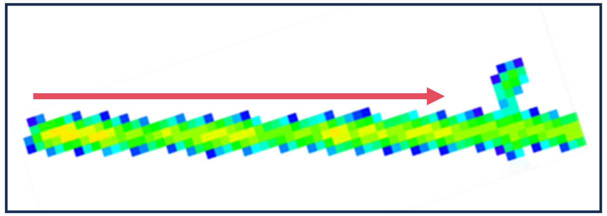

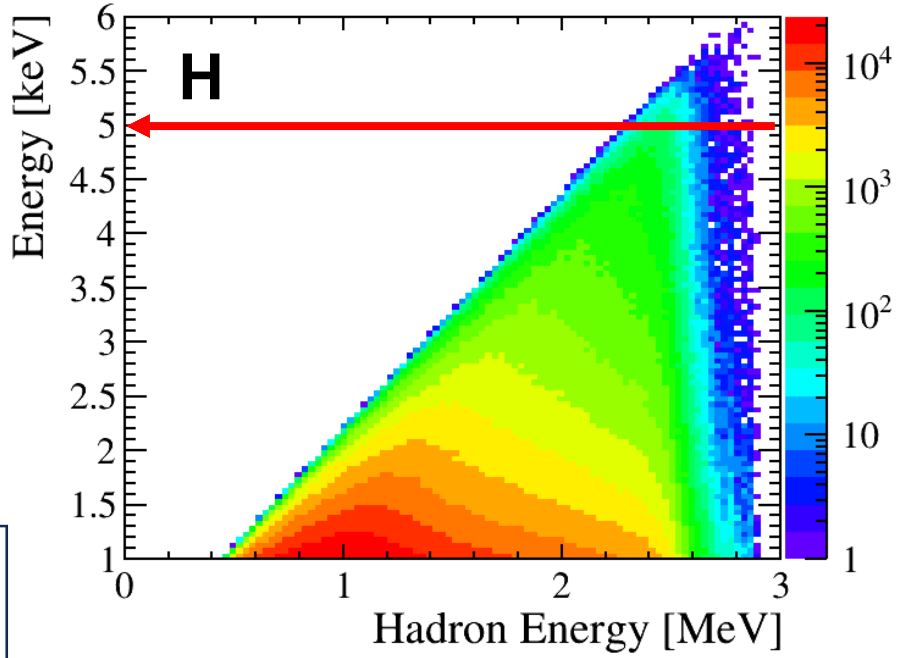

Only H has the **δ electron >** 5 keV.

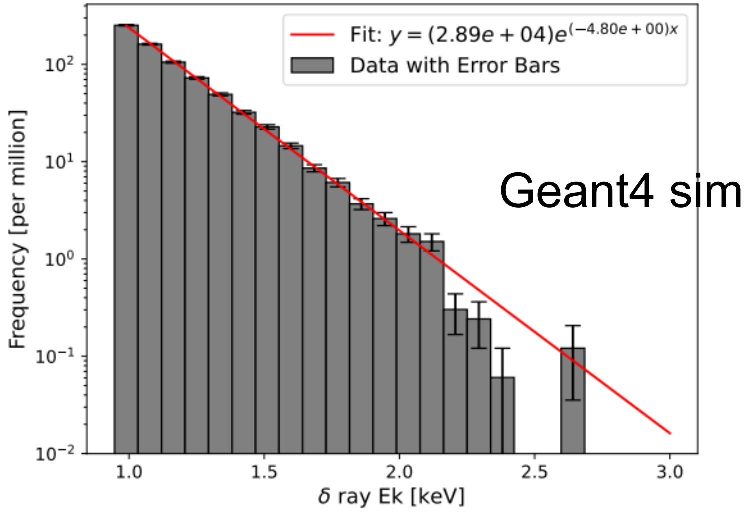

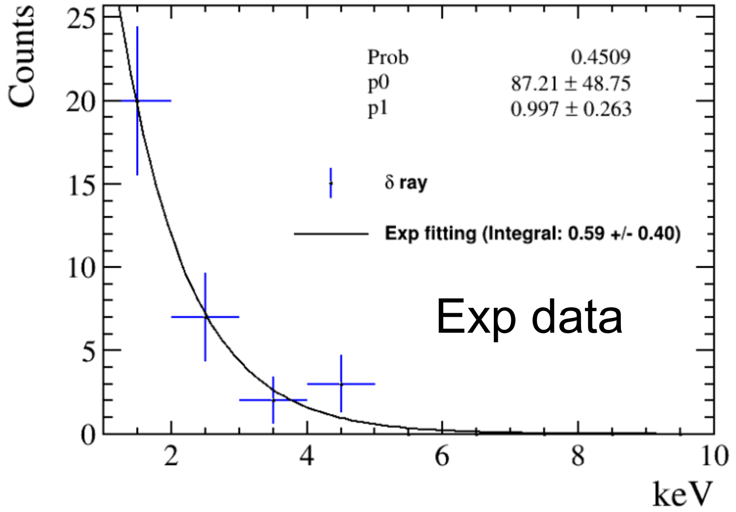

No δ above 5 keV were found.
Estimate by extrapolating from the exponential fit

- Consider the selection efficiency for δ-electrons.
- **Finally get: 0.035±0.023(stat.)**

Radom track conincidence

Method 1: n/γ spectrum measured by LS + GEANT4

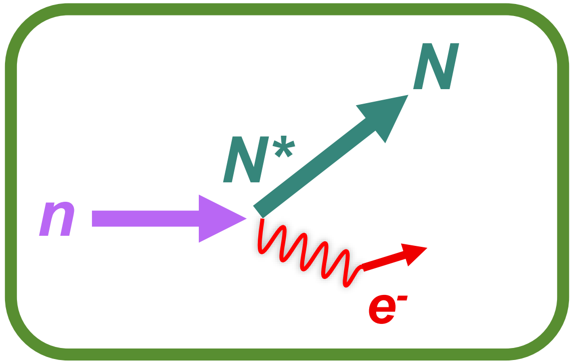

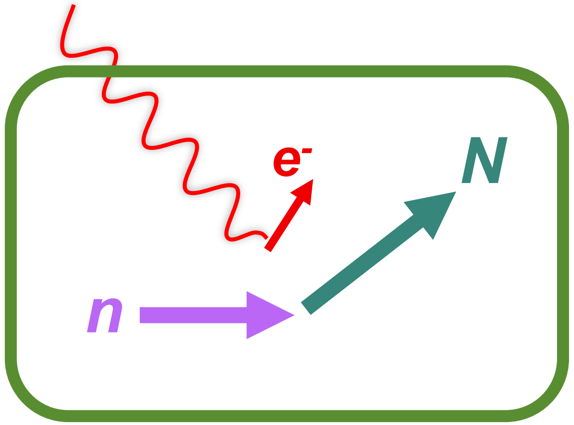

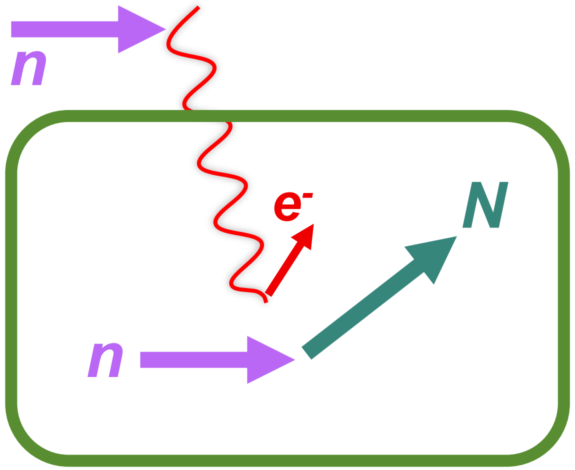

	NR	Compton e^-	photonEle
I	1	4.32×10^{-5}	1.06×10^{-5}
II	1	6.06×10^{-6}	$\sim 3.63 \times 10^{-8}$
III	1	3.11×10^{-6}	7.15×10^{-7}

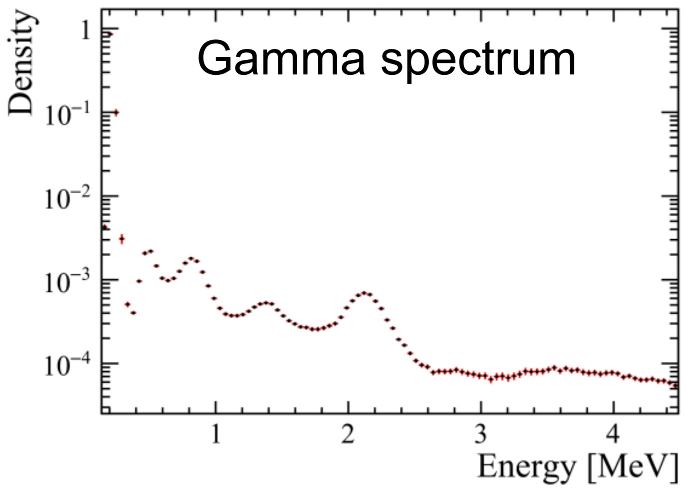

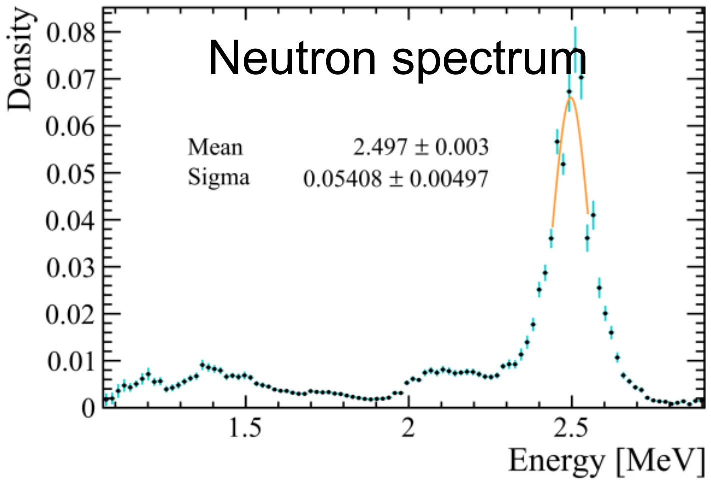

- **The expected background contribution of the 3 components in total is: 0.16±0.01(stat.)**

Radom track conincidence

- **Method 2: Estimated from Data**
  - Get the number of electron tracks within the 5-10 keV energy range that appear in the same frame as the nucleon tracks.
  - Considering the accidental coincidence of NR and ER with a vertex selection efficiency,
  - the final expected background value is **0.180±0.022(stat.)±0.042(sys.)**

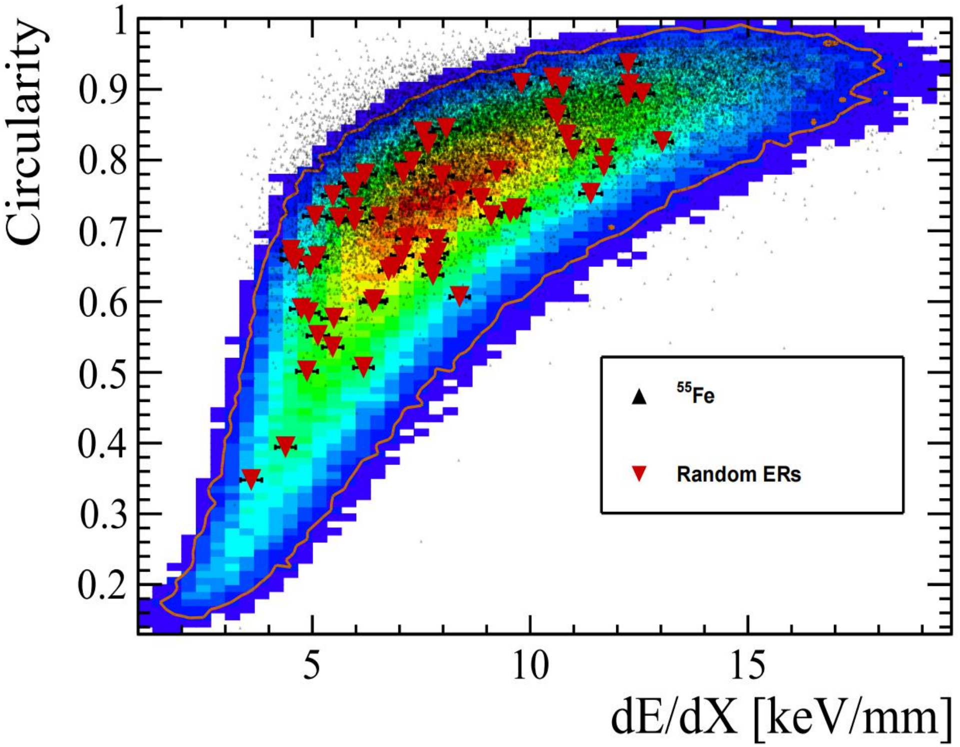

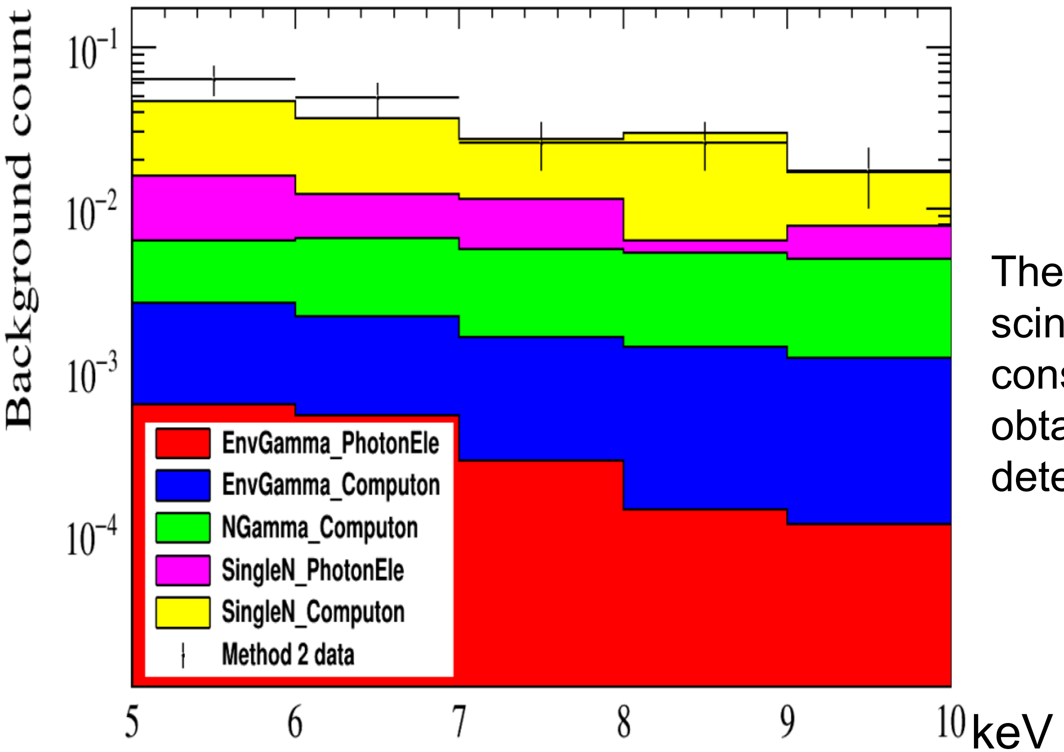

The results from the liquid scintillation + GEANT4 are consistent with the data obtained from the Migdal detector.

Cross section ratio calculation

MARVEL

- Probability: $P_{\mathrm{Migdal}}(5\mathrm{keV}<\mathrm{ER}<10\mathrm{keV},\ \mathrm{NR}>35\mathrm{keVee})=\dfrac{\left(\dfrac{n_{\mathrm{obs}}^{\mathrm{ER}}\text{-}n_{\mathrm{obs}}^{\mathrm{bg}}}{\varepsilon_{\mathrm{acc}}\varepsilon_{\mathrm{NR}}\varepsilon_{\mathrm{ER}}}\right)}{\left(\dfrac{n_{\mathrm{tot}}^{\mathrm{NR}}}{\varepsilon_{\mathrm{acc}}\varepsilon_{\mathrm{NR}}}\right)}=\dfrac{(n_{\mathrm{obs}}^{\mathrm{ER}}\text{-}n_{\mathrm{obs}}^{\mathrm{bg}})}{\varepsilon_{\mathrm{ER}}n_{\mathrm{tot}}^{\mathrm{NR}}}$
- Parameters:

	Efficiency/Count	Statistical Error	Systematic Error
Efficiency $\varepsilon_{\mathrm{ER}}$	14.4% 29%(YOLO)*49%(vertx rec)	±0.1%	±1.9%
$n_{\mathrm{tot}}^{\mathrm{NR}}$	8.17×10^5	±903	±35880
$n_{\mathrm{obs}}^{\mathrm{ER}}$	6		
$n_{\mathrm{obs}}^{\mathrm{bg}}$	0.229	±0.032	±0.043

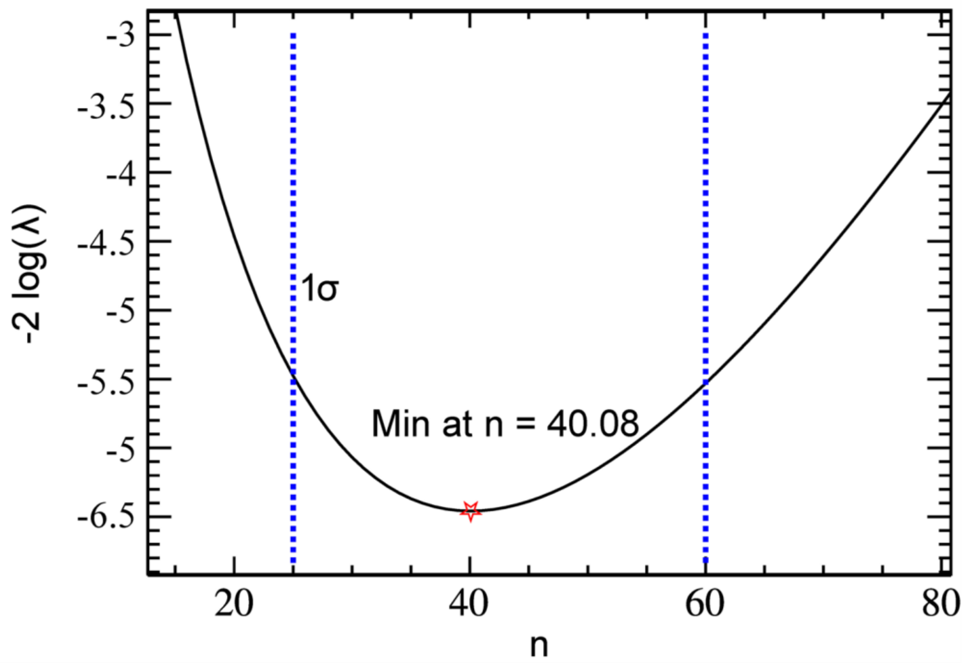

- upper/lower bounds: $\Delta P_{\pm} = \sqrt{\left(\dfrac{n_{min} - n_{ul/ll}}{n_{min}}\right)^2 + \left(\dfrac{n_{\mathrm{tot}\,\mathrm{error}}^{\mathrm{NR}}}{n_{\mathrm{tot}}^{\mathrm{NR}}}\right)^2} \cdot \dfrac{n_{min}}{n_{\mathrm{tot}}^{\mathrm{NR}}}$

Result: $4.9^{+2.6}_{-1.9} \times 10^{-5}$

Theory: 3.9×10^{-5}

The total transition probability

$$\sum_{nl} \frac{dp^i(nl \to E_e)}{dE_e}$$

The transition probability for ionization of an electron from an initial state (n, l) to a final state with energy E_e.

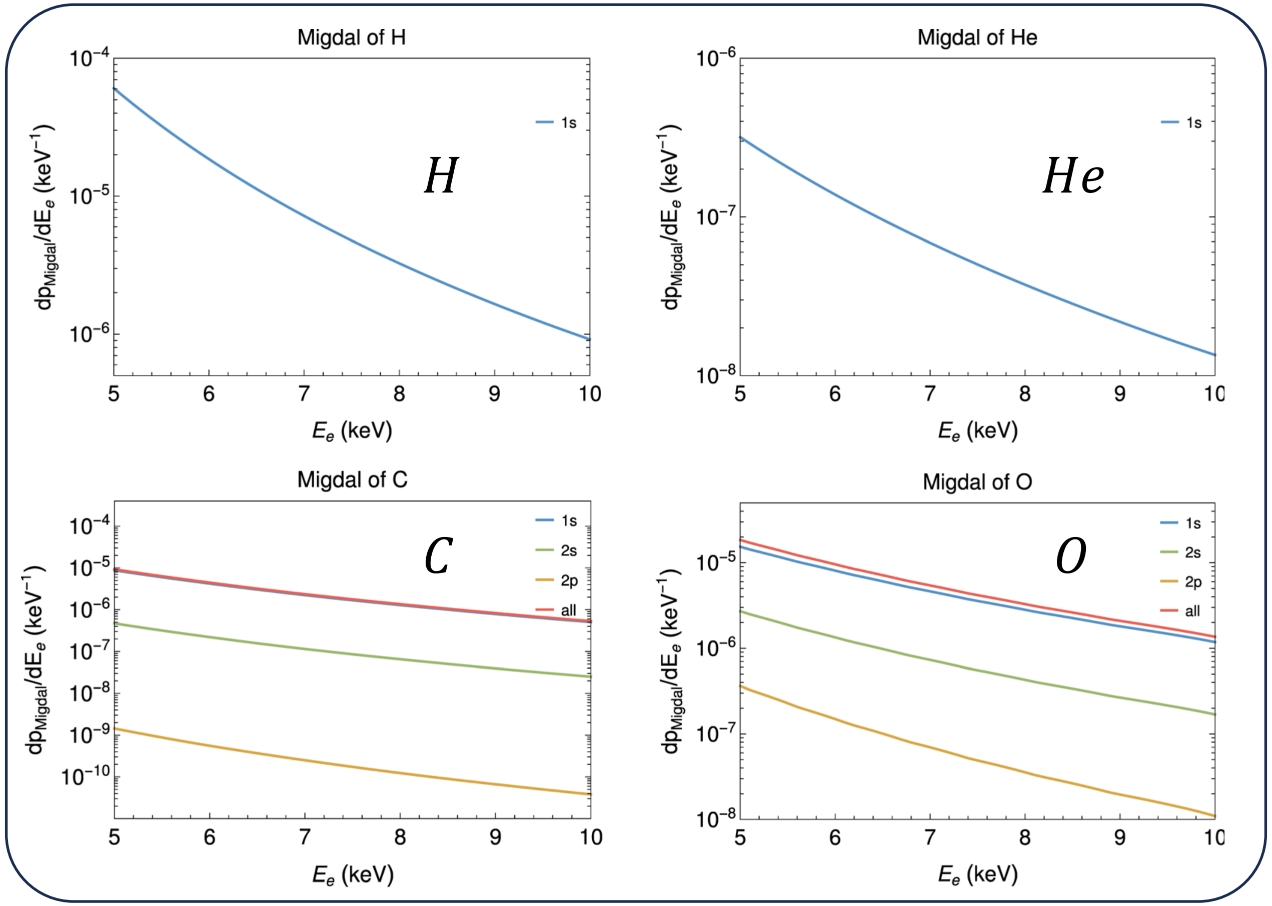

Transition probability of each element

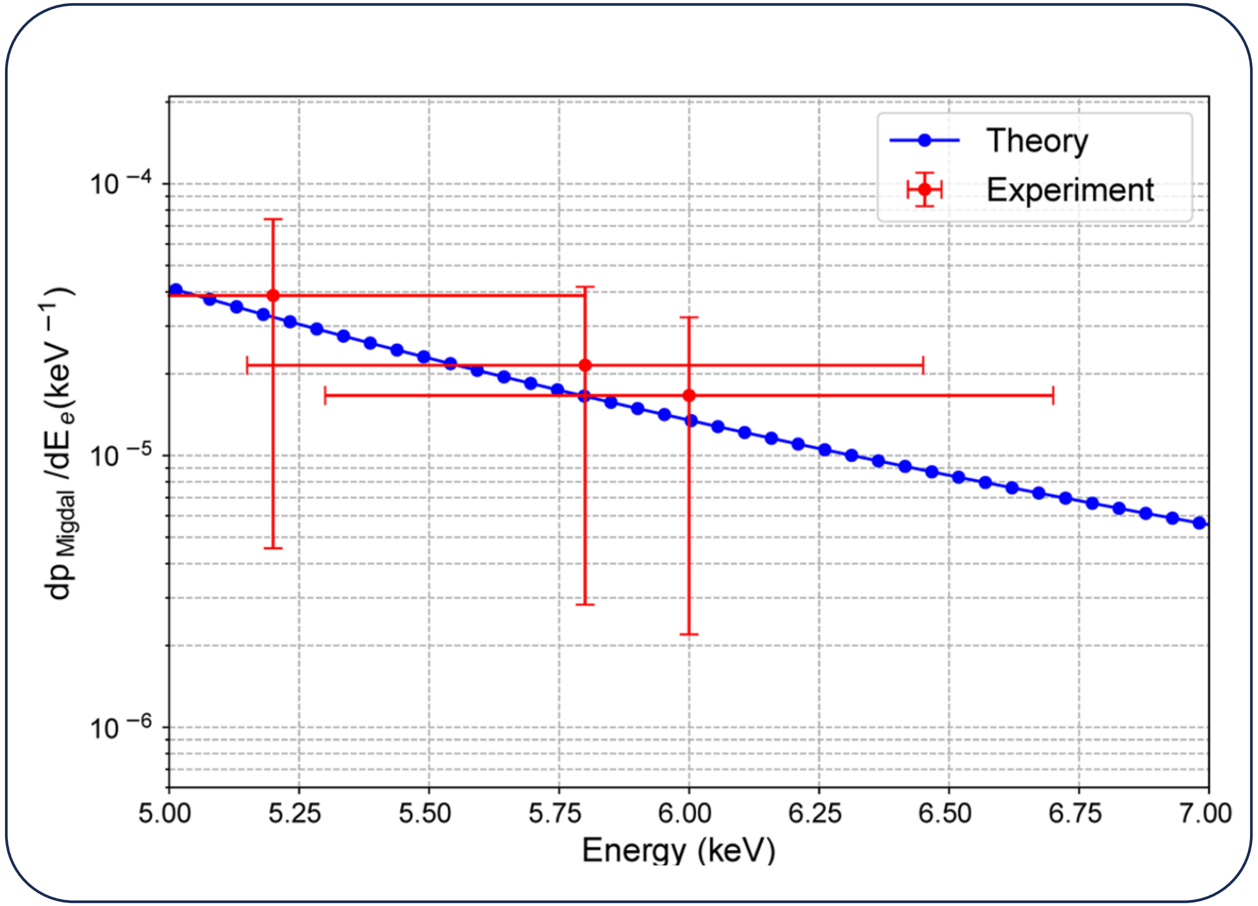

Total Transition probability

Upgrade in progress

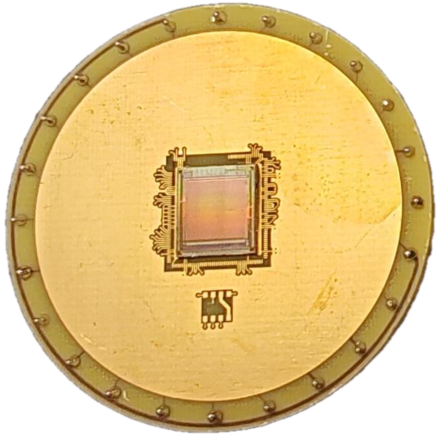

Topmetal-II

Topmetal-L

	Topmetal-II$^-$	Topmetal-L
Chip size [mm^2]	8×9	17×24
Active area [mm^2]	6×6	16.02×23.04
Pixel array	72×72	356×512
Pixel density [pixels/mm^2]	145	494
Power density [W/cm^2]	2.778	0.195
Pixel gain [μV/e$^-$]	-	76.04
ENC [e$^-$]	13.9	22.8
Readout mode	Rolling Shutter	Rolling Shutter / Sentinel
Time cost	2.6 ms/frame	0.73 ms/frame @ Sentinel

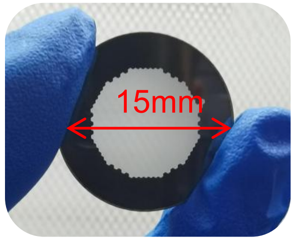

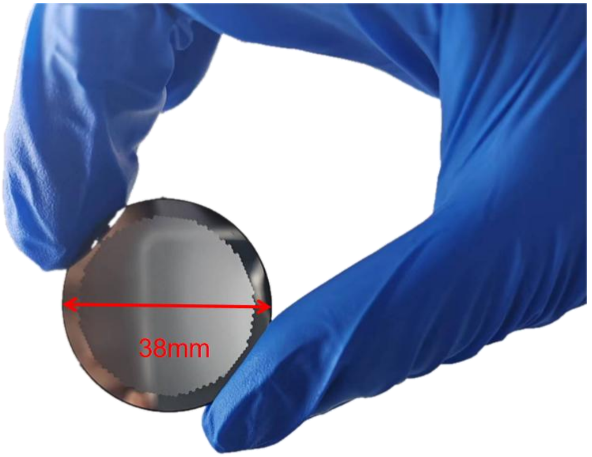

Larger GMCP

- 6x6 mm, 83 um in pitch -> 2.3x1.5 cm, 45 um in pitch
- Fresh time: 2.6 ms/Frame -> 0.7 ms/Frame
- Readout logic: Rolling Shutter -> Sensitive area

Upgrade in progress

Sensitive area readout:

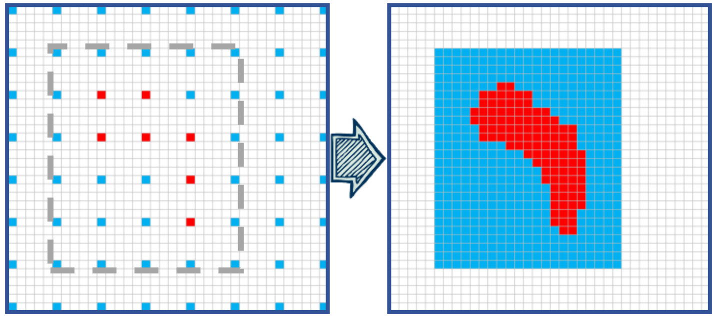

arXiv:2511.15130

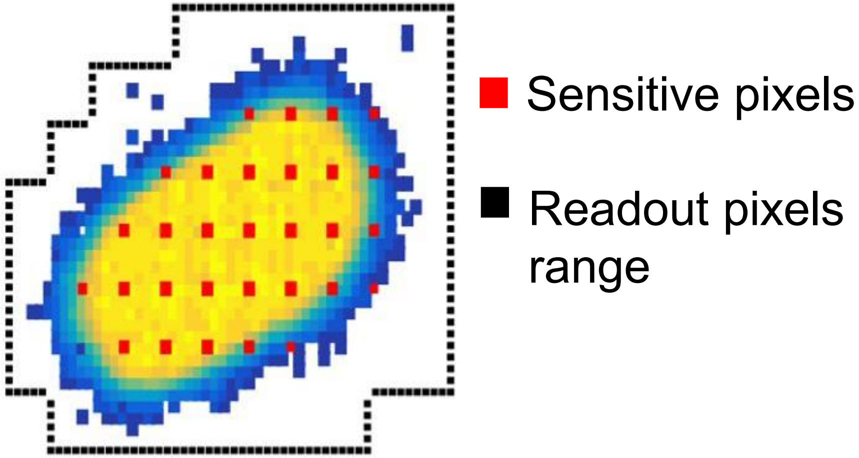

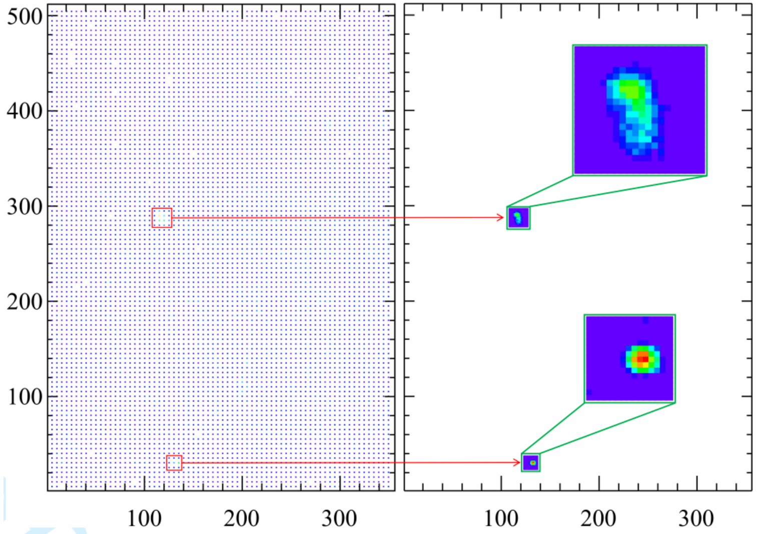

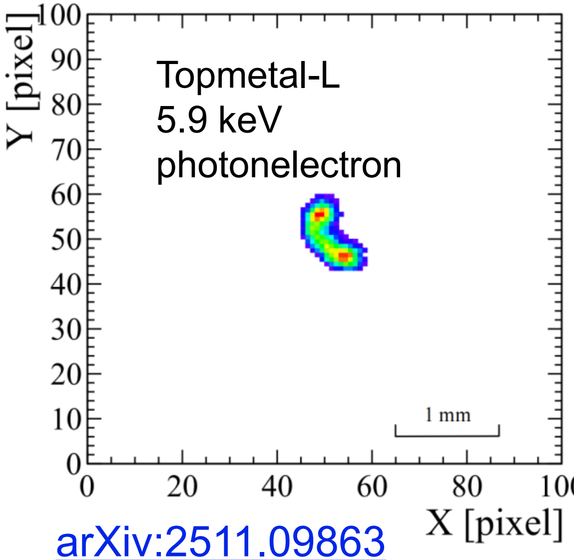

arXiv:2511.09863

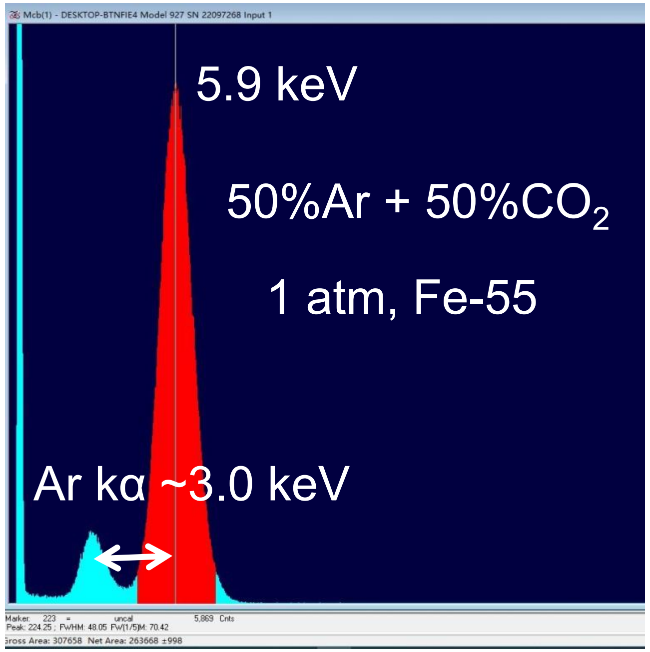

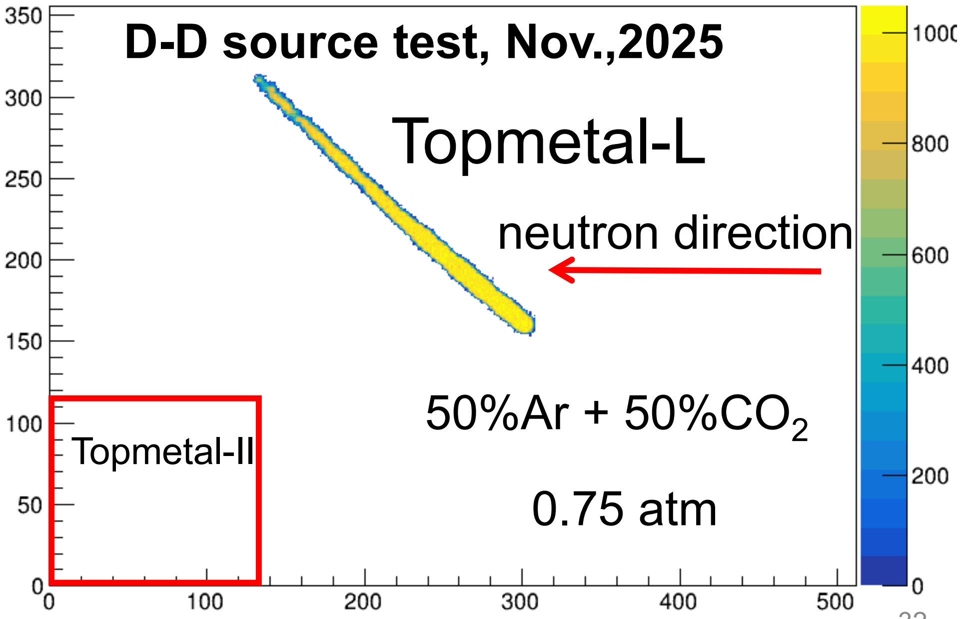

Upgrade in progress

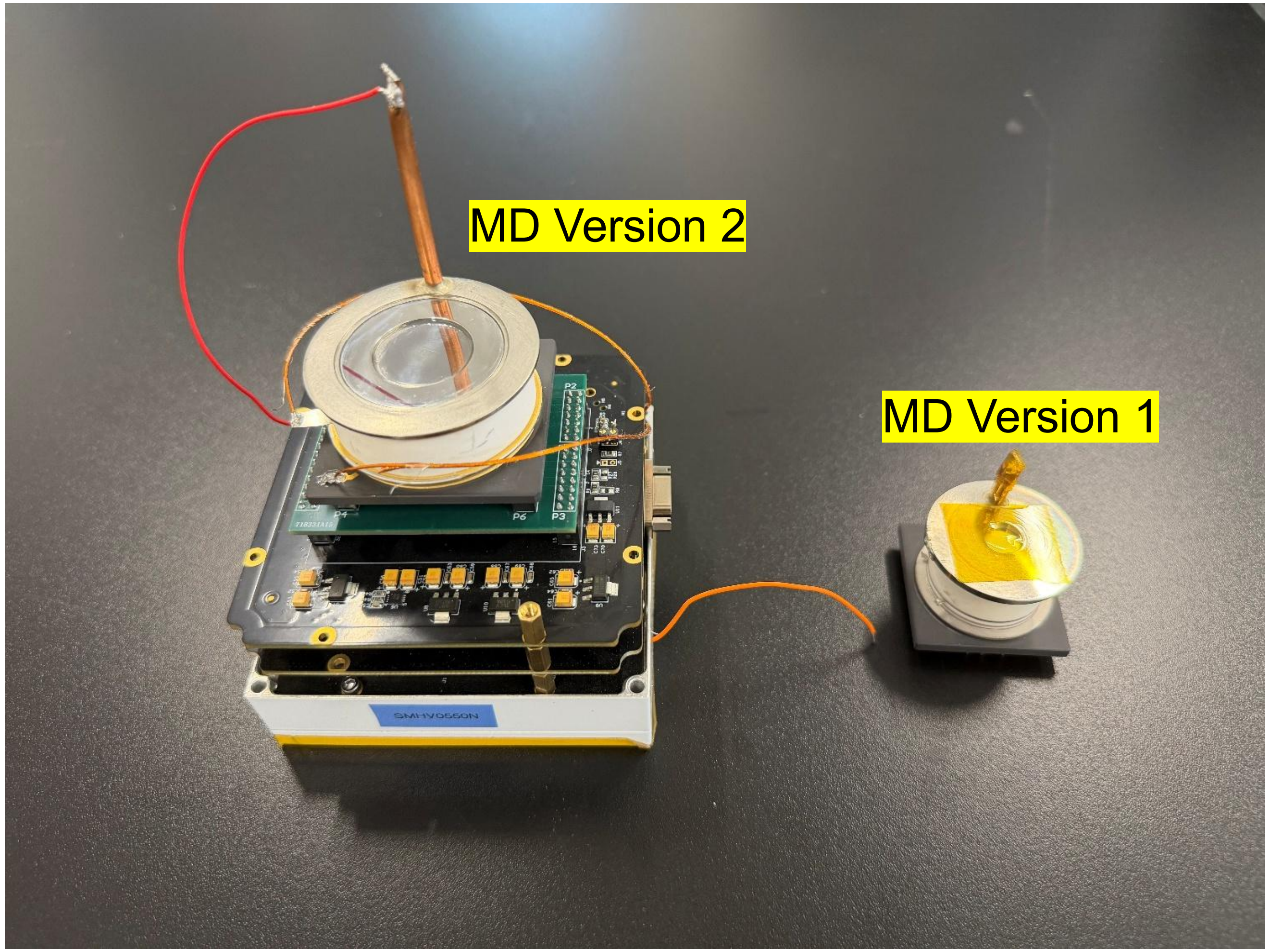

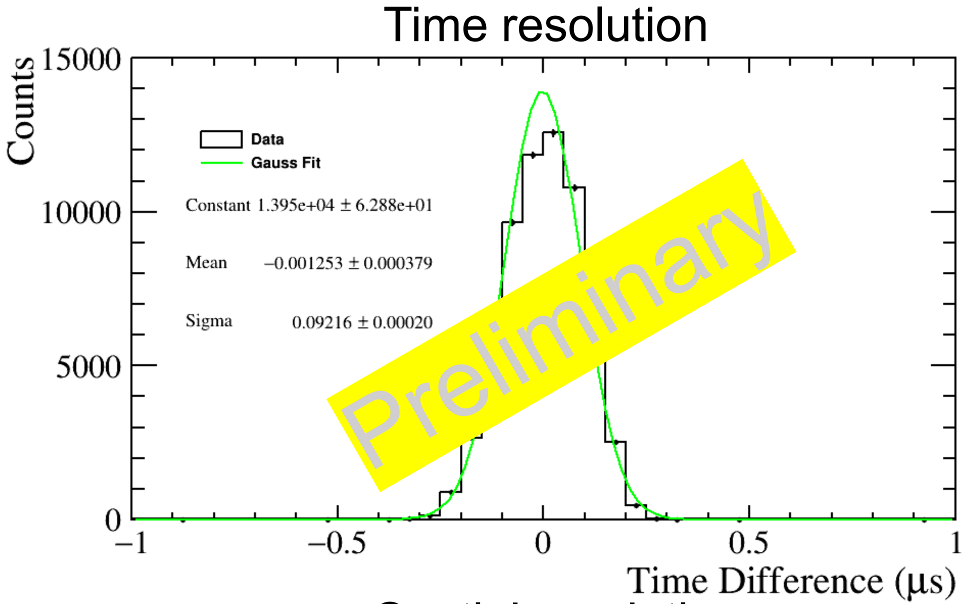

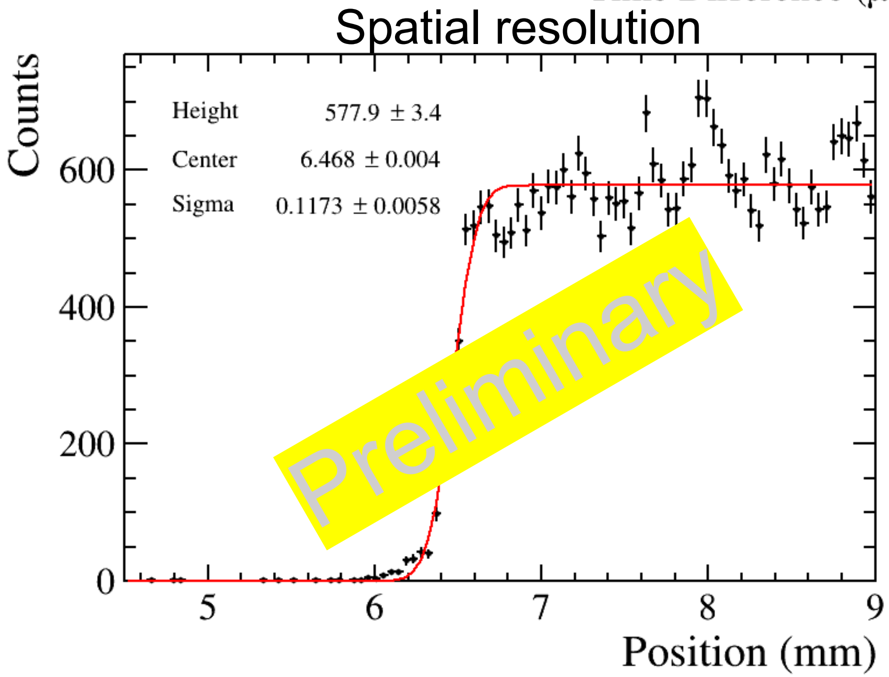

- The Migdal effect plays a very important role in sub-GeV dark matter research.
- The MARVEL experiment is dedicated to the direct detection of the Migdal effect.
- The ratio of the Migdal to the nuclear recoil cross-section to be $4.9^{+2.6}_{-1.9} \times 10^{-5}$, where nuclear recoils exceed 35 keVee and electron recoils span 5-10 keV.
- Detector upgrade is in progress.

Thanks for your attention!